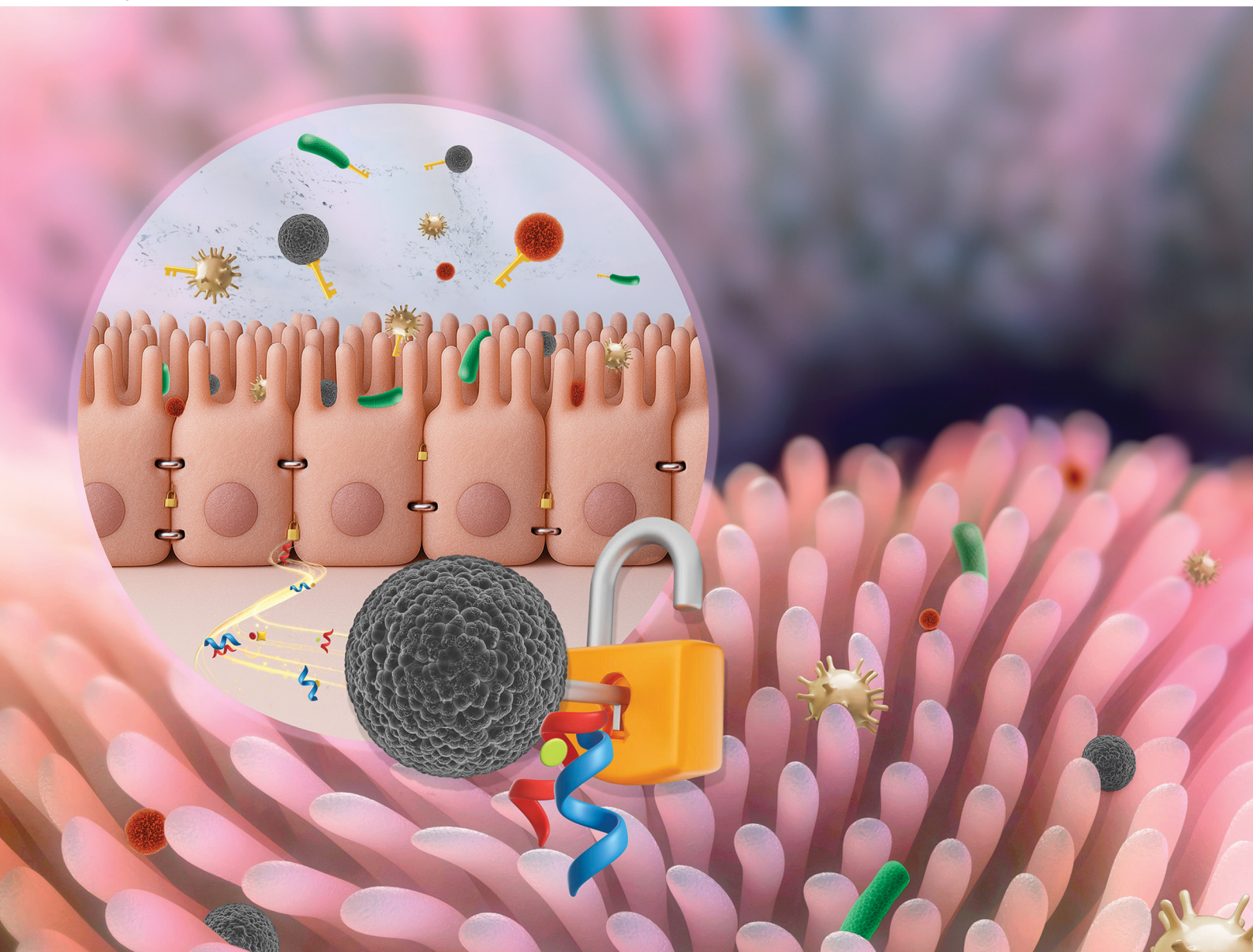


# NJC

New Journal of Chemistry  
rsc.li/njc

A journal for new directions in chemistry



ISSN 1144-0546

**PERSPECTIVE**

Claudia Iriarte-Mesa and Freddy Kleitz  
Tailored mesoporous silica nanoparticles for overcoming  
gastrointestinal barriers: a perspective on advanced  
strategies for oral delivery



Cite this: *New J. Chem.*, 2025, 49, 10018

Received 14th February 2025,  
 Accepted 21st April 2025

DOI: 10.1039/d5nj00654f

rsc.li/njc

## Tailored mesoporous silica nanoparticles for overcoming gastrointestinal barriers: a perspective on advanced strategies for oral delivery

Claudia Iriarte-Mesa <sup>ab</sup> and Freddy Kleitz <sup>\*a</sup>

Mesoporous silica nanoparticles (MSNs) offer new opportunities for the oral delivery of peptide drugs and biologics, owing to their biocompatibility and high drug-loading capacity. This perspective article explores strategies for the synthesis and functionalization of tailored MSNs, enabling precise control over particle size, morphology, and surface chemistry to overcome gastrointestinal barriers and enhance oral drug bioavailability.

One of the major challenges for the biopharmaceutical industry nowadays is to develop effective, safe, and patient-compliant medications while meeting complex regulations and current cost constraints. In this context, peptide drugs and biologics have revolutionized modern medicine by offering targeted therapies with high specificity and efficacy, resulting in

significant advances in the treatment of diseases such as diabetes, ulcerative colitis, and rheumatoid arthritis.<sup>1,2</sup> These medications have delayed or even reversed the course of immune-related conditions, changing the lives of people with chronic disorders, and offering hope for many patients who previously had no effective treatment options.<sup>3,4</sup>

Compared to small-molecule drugs, peptides and biologics have significantly higher molecular weights and inherently heterogeneous structures, which limit their solubility and oral bioavailability. However, in recent years, several attempts have been made to develop oral formulations of these compounds.<sup>5,6</sup>

<sup>a</sup> Department of Functional Materials and Catalysis, Faculty of Chemistry, University of Vienna, 1090 Vienna, Austria. E-mail: freddy.kleitz@univie.ac.at

<sup>b</sup> Vienna Doctoral School in Chemistry (DoSChem), University of Vienna, 1090 Vienna, Austria



**Claudia Iriarte-Mesa**

*Claudia Iriarte-Mesa is a Post-doctoral Research Assistant at the University of Vienna, Austria. She received her Bachelor's degree in Chemistry in 2016 and her Master's degree in 2018 from the University of Havana, Cuba. Her research at the Department of Bioinorganic Chemistry, University of Havana, focused on the conjugation of biomolecules to functional inorganic nanomaterials, including iron oxide, copper sulfide, and gold nanoparticles, for environmental and biomedical applications. In 2019, she joined the Department of Functional Materials and Catalysis of the University of Vienna, Austria, as a research assistant and PhD student under the supervision of Prof. Dr Freddy Kleitz. She received her doctorate degree (Dr rer. nat.) in Chemistry in 2024, with a focus on designing mesoporous silica materials for the oral delivery of peptide drugs and biologics.*



**Freddy Kleitz**

*Freddy Kleitz is a University-Professor in the Faculty of Chemistry at the University of Vienna, Austria. Since 2016, he has been the director of the Department of Functional Materials and Catalysis. He received his doctorate degree (Dr rer. nat.) in Chemistry in 2002 from the Max-Planck-Institut für Kohlenforschung and the Ruhr University Bochum, Germany. In 2002–2003, he was a postdoctoral researcher at KAIST in South Korea. In 2005, he joined the Department of Chemistry of Université Laval, Canada, where he was awarded the Canada Research Chair on Functional Nanostructured Materials. He was then promoted to the rank of Full Professor in 2014. His research focuses on the design of functional nanoporous inorganic and organic–inorganic hybrid materials, and their applications as selective sorbents, heterogeneous catalysts, and biomedical materials.*



Oral administration tackles the significant disadvantages associated with the parenteral route, such as pain and discomfort, severe reactions at the injection site, scarring, local allergic reactions, and cutaneous infections. These effects can lead to poor patient adherence when long-term follow-up and repeated dosing are necessary.<sup>7</sup>

Despite its benefits, oral delivery of macromolecules remains challenging due to the obstacles generated by the gastrointestinal (GI) system. As large and complex molecules, biologics are susceptible to the harsh GI milieu, including the acidic environment in the stomach, digestive enzymes, and microbiota, which play pivotal roles in digestion.<sup>5,6</sup> Although it is possible to ensure protection against degradation, most of these drugs cannot pass through the intestinal mucus due to their large size. Systemic oral delivery of biologics and peptide drugs is additionally prevented by the intestinal barrier, in which intercellular tight junction complexes block their passage to the bloodstream.<sup>8,9</sup>

After nearly a century of research aimed at achieving oral delivery of macromolecules, the current clinical reality remains unchanged, mainly in terms of therapeutic administration. Along with the latest advances in materials science, research on peptide drugs and biologics is yielding clinically relevant drug delivery technologies, making oral administration a viable option for the near future.<sup>10</sup> Some of the alternative systems are based on the use of permeation enhancers, enzyme inhibitors, and mucus-penetrating and cell-penetrating peptides.<sup>11</sup> However, nanoparticle-based formulations exhibit a unique potential in drug delivery applications. Such carriers have been demonstrated to overcome physicochemical barriers in the gut, providing controlled release, novel transport mechanisms, and improved oral bioavailability of payloads.<sup>12</sup> A large amount of research on the oral delivery of macromolecules using nanomaterials has focused on lipids, liposomes, polymer conjugates, and dendrimers.<sup>7</sup>

Owing to their nanometer-scale size, mesoporous silica nanoparticles (MSNs) can safely penetrate the intestinal epithelium while carrying their protected cargoes.<sup>6,13</sup> Specifically, dendritic (*i.e.*, dendrimer-like) MSNs (DMSNs) offer customizable pores in the range of 6–45 nm, large enough to host high-molecular-weight drugs, combined with an almost monodispersed particle size distribution in the range of 50–150 nm, which is suitable for navigating through the intestinal barrier. Especially for peptide delivery, DMSNs have been shown to provide all the ideal benefits as drug carriers. The small particle size and tunable large pores, along with a negatively charged surface, have enabled simultaneous high loading and efficient interaction with the intestinal epithelium.<sup>14</sup>

The optimization of MSN morphology, particle size, surface charge, and porosity has been extensively studied to improve the efficacy of MSN-based systems for oral drug delivery. However, prior to clinical developments, oral formulations still must be optimized in terms of drug loading efficiency, retention of biological activity of the cargoes after encapsulation, and protection against proteolysis.<sup>6</sup> In this regard, the functionalization of the MSNs carriers has offered significant advantages in oral delivery.<sup>15</sup> By tuning the surface chemistry of these materials, the interaction of confined drugs with silica has been additionally improved,

ensuring controlled release and enhanced performance in gastrointestinal conditions.<sup>16</sup> Tailored functionalization has enabled the selective loading of large biomolecules, such as enzymes, while retaining their biological activity and even enhancing their catalytic performance.<sup>17</sup>

MSNs have shown promise as nanocarriers in oral formulations. However, challenges related to colloidal stability, intestinal permeability, and mucoadhesion must be addressed to improve the delivery of peptide drugs and biologics and achieve meaningful therapeutic outcomes *in vivo*. Additionally, understanding particle biodistribution, clearance mechanisms, and long-term safety is essential for the clinical translation of MSN-based formulations.<sup>6,13,18</sup>

This perspective article explores strategies for the synthesis and functionalization of MSNs, specifically designed to get through GI barriers that limit the efficacy of oral formulations, including the mucus layer and the tight intestinal epithelium. Approaches to diversifying MSN morphology, particle size, and surface chemistry are discussed, along with recent studies correlating these properties with the interaction of MSNs with intestinal cells, their diffusion through the mucus, and the modulation of the intestinal barrier. This overview highlights the unique potential of MSNs as nanocarriers for oral drug delivery, emphasizing their role in reducing mucus trapping and enhancing intestinal permeability. Additionally, it provides guidelines for their tailored design and advanced testing of the particle performance in contact with intestinal cells.

## 1. Physiological barriers in the gut and MSNs in oral drug delivery

The complex architecture of the GI tract supports essential biological functions, including nutrient digestion, absorption, and waste elimination. Beyond mechanical and chemical processing of food, it also protects the body by defending against pathogens and regulating selective uptake.<sup>19</sup> Consequently, physicochemical barriers such as the gastric and intestinal digestive environment, the mucosal lining, and the tightly packed intestinal epithelium can hinder the transport of orally administered drugs and their entry into the systemic circulation (Fig. 1).<sup>4,7,20</sup>

Drug loading into MSNs, designed to tackle some of these barriers, along with strategies for silica functionalization, has enabled the development of formulations with potential applications for oral delivery. These formulations ensure low toxicity and minimal disruption to the intestinal barrier function.<sup>21–24</sup>

The following sections provide an overview of the mucosal barrier, the tight intestinal epithelium, and the pathways that mediate absorption and subsequent systemic delivery of orally administered drugs. Additionally, the impact of the physicochemical properties of MSNs on their biological performance in the gastrointestinal compartment is discussed.

### 1.1. The mucosal barrier

The intestinal mucus barrier is composed of water, mucin glycoproteins secreted by goblet cells, ions, enzymes, and



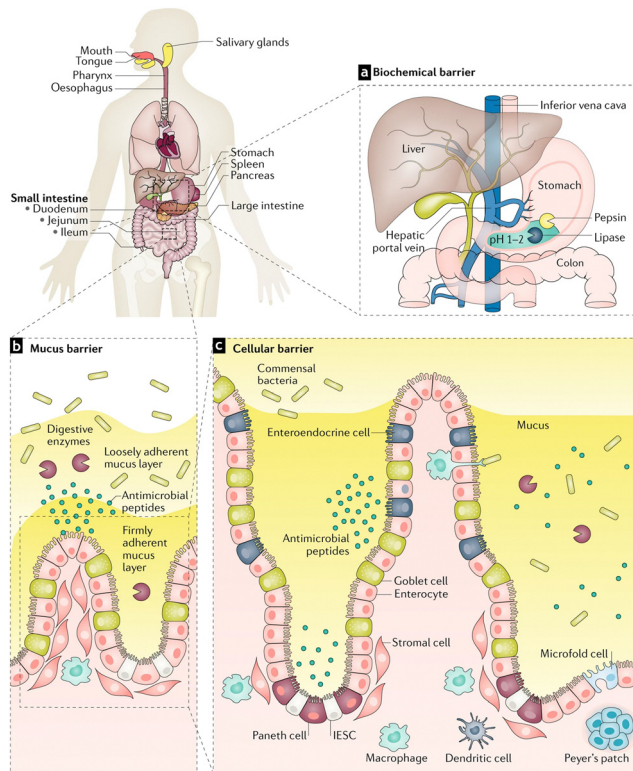


**Fig. 1** Physiological barriers in the gastrointestinal compartment limiting oral delivery of peptide drugs and biologics: (a) biochemical barrier including the acid environment in the stomach and digestive enzymes, (b) mucus barrier, and (c) cellular barrier corresponding to the tight intestinal epithelium. Adapted with permission.<sup>4</sup> Copyright © 2019, Springer Nature.

immunoglobulins. These elements form dense layers, shielding the epithelium from mechanical harm, pathogens, and chemical damage. The thickness of mucus varies from the stomach (30–300  $\mu\text{m}$ ) to the small intestine (150–400  $\mu\text{m}$ ) and the colon (30–280  $\mu\text{m}$ ), limiting the passage of nanomaterials.<sup>25</sup> Indeed, it has been reported that the crosslinked mucin fibers of the mucus only allow the diffusion of particles smaller than 200 nm. However, if particles are too small, they risk being rapidly cleared from the body before they can cross the intestinal epithelium.<sup>26</sup> Therefore, optimizing the particle size is crucial to ensure mucus penetration and retention within the GI tract.<sup>27</sup>

The mucus surface is mostly negatively charged due to the carboxyl and sulphate groups of mucins. This, along with the hydrophobic nature of lipid moieties in proteoglycans, hinders the diffusion of hydrophobic or positively charged MSNs.<sup>25</sup> Accordingly, functionalization of the silica surface has been used to minimize particle interactions with the mucus layer, allowing neutral or negatively charged MSNs with hydrophilic grafted moieties, such as polydopamine, polyethylene glycol (PEG), and zwitterion functions, to transit smoothly and escape rapid clearance.<sup>28</sup>

Furthermore, the morphology of MSNs influences their ability to navigate the mucus. Several studies have shown that

nanorods traverse this barrier more efficiently than spherical particles. This is because elongated shapes provide a dynamic orientation that reduces the effective size in contact with mucus, allowing the particles to slip through its dense network more efficiently.<sup>29</sup>

In addition to morphology, the role of surface roughness in particle trafficking through the mucus layer has been investigated. In this context, virus-like MSNs have been synthesized to mimic the size and shape of biological viruses, enabling more efficient penetration and transport within the mucus. For example, Zhang *et al.* developed virus-like MSNs that significantly reduced binding to mucin compared to smooth particles, thereby ensuring faster penetration through the mucus layer and improving permeability across the epithelium for the oral delivery of insulin.<sup>30</sup>

## 1.2. The intestinal epithelial barrier: paracellular and transcellular pathways

Once the mucus barrier has been crossed, nanomaterials are either taken up intracellularly or interact with the intestinal cells, privileging the paracellular route by loosening the cell junctions.<sup>31,32</sup> The intestinal barrier comprises various types of cells, such as enterocytes, goblet cells, and enteroendocrine cells, closely joined by such tight junction proteins (TJs) that modulate selective permeability through the epithelium. Additionally, the mucosal linings secreted by goblet cells provide protection against pathogens while facilitating the passage of nutrients and drugs through both transcellular and paracellular pathways.<sup>33</sup>

Paracellular transport refers to the passage of substances across intestinal cells, regulated by TJs such as claudins, occludin, and zonula occludens. These proteins regulate the permeability of the epithelial layer, allowing for the selective passage of small molecules, water, and ions. However, its restrictive selectivity generally limits the passage of large molecules, posing challenges for delivering larger therapeutic compounds and biologics.<sup>8,9</sup> This selectivity underscores the importance of potentially modulating TJ dynamics to enhance the efficiency of oral formulations.<sup>34,35</sup>

The interaction of MSNs with epithelial cells can disrupt TJs, increasing intestinal permeability.<sup>36,37</sup> Lamson *et al.* used MSNs to deliver insulin and exenatide in diabetic mice through TJ modulation.<sup>38</sup> Smaller particles (20–200 nm) facilitated MSN diffusion through the mucus, while their highly negative surface charge (−40 to −80 mV) further enhanced the permeability of Caco-2 monolayers. The authors postulated the interaction of MSNs with apical integrins, stimulating pathways that lead to the phosphorylation of myosin light chain kinase (MLCK). Such a phosphorylation process is crucial in regulating barrier function as it can induce actomyosin contraction and subsequent reorganization of the epithelium architecture.<sup>31,39</sup> Accordingly, these studies confirmed zonula occludens-1 (ZO-1) redistribution and overall depletion of the TJs.<sup>38</sup>

Furthermore, the interaction of MSNs with TJs has been enhanced by proper functionalization of the silica surface. Thus, permeation enhancers such as peptides, chitosan, thiolated



polymers, and fatty acids have been conjugated to MSNs to transiently modulate TJ proteins without damaging the barrier integrity while increasing paracellular permeability.<sup>7</sup> TJ disruption may lead to increased susceptibility to infections and the systemic absorption of harmful substances.<sup>34</sup> Thus, compounds that alter intestinal barrier function by modifying the organization and fluidity of the cell membrane, altering TJ expression, or inhibiting endocytosis are frequently used to elucidate the pathways involved in the interaction of nanomaterials with intestinal cells while confirming the material safety, integrity of the cell monolayer, and transient disruption of the barrier.<sup>40–42</sup>

The transcellular route is, in turn, a less invasive pathway that facilitates the transport of nanoparticles across the intestinal barrier, enabling the direct movement of substances through cells. This typically occurs *via* membrane-bound carriers or passive diffusion, which are essential for nutrient uptake and waste elimination.<sup>43</sup> Endocytosis, a specific form of transcellular transport, involves the enveloping of extracellular material by the cell membrane, which forms vesicles that transport these compounds or particles into the cells. This pathway is crucial for the uptake of larger molecules, such as proteins and lipids, which cannot cross the cell membrane directly.<sup>44</sup>

The internalization mechanisms are divided into phagocytosis, pinocytosis, and receptor-mediated endocytosis.<sup>40</sup> Phagocytosis is typically used to capture and eliminate pathogens, involving the encapsulation of large particles.<sup>45</sup> On the other hand, pinocytosis is a process in which intestinal cells internalize extracellular fluid and small solutes through small vesicles, allowing the cell to adjust to its environment.<sup>46</sup> In turn, receptor-mediated endocytosis is a more selective pathway that involves specific binding of cell surface receptors to external matter, triggering vesicle formation and subsequent internalization. Such pathways include clathrin- and caveolin-mediated endocytosis, both of which have been widely explored for the cellular uptake of nanocarriers in drug delivery.<sup>40</sup>

The physicochemical properties of MSNs can significantly influence their cellular uptake. Thus, the modification of silica charge, size, morphology, and chemical surface has been explored to enhance transcellular transport and internalization of drug cargoes.<sup>21</sup> For example, Zheng *et al.* described the effect of morphology on endocytosis-mediated uptake.<sup>47</sup> The authors finely tuned the reaction conditions to diversify the aspect ratio of MSNs, obtaining spherical and rod-like particles with identical surface chemistry. Mechanistic studies with endocytosis inhibitors demonstrated that while the nanorods were internalized *via* a caveolae-mediated pathway, the clathrin receptors contributed to the uptake of spherical MSNs. Additionally, it has been reported that smaller MSNs (< 50 nm) with a surface charge between +15 and –15 mV undergo receptor-mediated endocytosis, which facilitates endolysosomal escape and targeting toward mitochondria, the endoplasmic reticulum, and the Golgi apparatus.<sup>48</sup>

The surface chemistry of the nanoparticles has also been modified to enhance interaction with intestinal cells, privileging

endocytic pathways.<sup>15</sup> For example, it has been demonstrated that functionalization with positively charged groups or amphiphilic copolymers can enhance interactions with lipid headgroups of the membrane, thereby favoring internalization and improving the bioavailability and therapeutic efficacy of the transported drugs.<sup>49,50</sup>

## 2. Strategies for the synthesis and functionalization of MSNs

The physicochemical properties of MSNs play a crucial role in the performance of such materials as nanocarriers in oral delivery applications, significantly influencing drug loading, release kinetics, mucus penetration, intestinal permeability, and overall oral bioavailability.<sup>26</sup> This section describes strategies for the synthesis and functionalization of MSNs, enabling precise control over particle size, morphology, surface roughness, and organic functions anchored to the silica surface, which offers valuable tools for designing MSNs with tailored performance in the GI compartment.

The synthesis of mesoporous materials involves sol-gel reactions wherein silica polymerization is conducted around the micelles. This process is based on the cooperative self-assembly between structure-directing agents, such as surfactants or block copolymers, and inorganic silica precursors, including organosilanes, which occurs in an aqueous alcoholic solution, typically ethanol, used to dissolve both organosilanes and surfactants.<sup>51</sup> Cationic surfactants such as cetyltrimethylammonium bromide (CTAB) or cetyltrimethylammonium chloride (CTAC) are widely used as structure-directing agents. At the same time, tetraethoxysilane (TEOS), tetramethoxy silane (TMOS), and sodium silicate are the most common silica precursors in the synthesis of mesoporous materials.<sup>52</sup>

Initially, the surfactant self-assembles into micellar structures when its concentration reaches the critical micellar concentration.<sup>51</sup> Experimental conditions, such as pH, temperature, and surfactant concentration, directly influence the shape and size of the micellar arrangement formed, which is essential for inducing and diversifying the porosity of the products.<sup>53</sup> Then, the inorganic precursor is catalytically hydrolyzed to form silanol groups (Si–OH) and further condenses into polymeric silica-based species, generating siloxane bonds (Si–O–Si) that align around the micellar arrangement through supramolecular templating.<sup>54</sup> This sol-gel process leads to the growth of the silica network and is facilitated by acidic (*e.g.*, HCl) or base catalysts such as NH<sub>4</sub>OH, NaOH, triethanolamine (TEA), or diethanolamine (DEA), which significantly influence the rate of hydrolysis and condensation reactions (Fig. 2).<sup>52</sup>

MSNs are typically synthesized at low temperatures, ranging from 25 °C to 80 °C. Consequently, the mesoporous structure should be consolidated through hydrothermal treatment (80–150 °C) or aging to achieve complete condensation of the silica framework. Although not mandatory, these post-synthetic procedures are commonly used to enhance the ordering of the resulting particles, thereby favoring pore expansion and



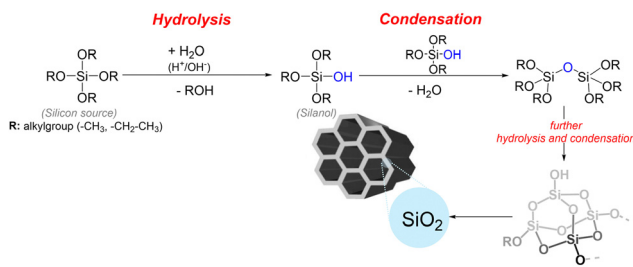


Fig. 2 Schematic representation of the reactions involved in the synthesis of mesoporous silica.

improving hydrothermal stability.<sup>55</sup> The mesopores are finally generated after removing the surfactant template either by solvent extraction or calcination.<sup>52</sup> Calcination must be performed for several hours at temperatures above 500 °C in the presence of oxygen to eliminate the organic species through thermal decomposition.<sup>56</sup> On the other hand, extraction with organic solvents enables the removal of templates while preserving organic functional groups within the silica matrix, which is essential for the subsequent applications of these materials.<sup>57</sup> For this purpose, extraction with an EtOH/HCl mixture under refluxing conditions is typically used to reduce electrostatic interactions between the positively charged head groups of the surfactants and the silicate anions.<sup>58</sup> The extraction process should be repeated several times or combined with sonication to enhance the efficiency of template removal. Furthermore, the choice of solvent should be made according to the specific template, and its total removal is not always guaranteed.<sup>59</sup>

The first synthesis of MSNs was reported by Grün *et al.* in 1997.<sup>60</sup> Colloidal particles, ranging from 400 to 1100 nm, were obtained by modifying the Stöber synthesis, which involves the hydrolysis and condensation of TEOS in a mixture of ethanol and water containing ammonia as a base catalyst.<sup>61</sup> The addition of cationic surfactants to the reaction mixture provided the micelles needed to form spherical MCM-41 particles with pore diameters ranging from 2.9 to 3.6 nm.<sup>60</sup> The original procedure, developed by Werner Stöber and colleagues in 1968, successfully produced non-porous, spherical particles with a uniform size distribution in the micron-size range.<sup>62</sup> Furthermore, when combined with the cooperative self-assembly mechanism, the Stöber-based protocol allowed the generation of porosity with precise control over the morphology, pore size, particle size, and surface properties of the MSNs.<sup>52,63</sup> The fine-tuning of reaction conditions has produced tailored particles with nanometric sizes suitable for a wide range of applications.<sup>64,65</sup>

### 2.1. Control of particle size and colloidal aggregation

The size of the MSNs is critical when targeting specific biological applications. Precise control over particle dimensions ensures efficient drug delivery, optimal biodistribution, effective interactions with cells and tissues, and effective blood circulation and clearance from the body.<sup>66–68</sup>

The pH of the reaction affects both the hydrolysis and condensation of the silica precursor and the micellar organization

of the surfactant, being a critical factor that controls the nucleation and growth of MSNs. Thus, the production of large particles, such as MCM-48 and MCM-41 MSNs, can be achieved by increasing the concentration of the base catalyst.<sup>63</sup> Furthermore, Zainal *et al.* reported that increasing the reaction temperature from 30 °C to 70 °C resulted in particle growth from 30 nm to approximately 115 nm.<sup>69</sup> This effect can be attributed to the acceleration of the reaction rate, which favors the polycondensation of silica. Since it is known that organic co-solvents facilitate the solubilization of various species within the reaction medium and influence the reaction rate, micelle assembly, and colloidal aggregation,<sup>70,71</sup> a similar trend was observed with the addition of butanol, which increased particle size from *ca.* 45 nm to 105 nm.<sup>69</sup> On the other hand, additives such as alcohols, amines, inorganic bases, and inorganic salts also alter the hydrolysis and condensation of the silica precursor, accelerating the reaction kinetics and leading to the formation of smaller particles.<sup>52</sup> For example, Möller *et al.* used TEA instead of NaOH or  $\text{NH}_4\text{OH}$  to generate small particles (below 150 nm) with narrow size distributions.<sup>72</sup> Similarly, Bouchoucha *et al.* reported the production of well-dispersed MSNs using TEA as a base catalyst, which additionally acted as a complexing agent, limiting particle growth.<sup>73</sup>

It is known that when the size of MSNs is reduced, the aggregation rate increases because the particles interact with each other to attenuate their surface tension.<sup>53</sup> In this context, using L-lysine as a moderate catalyst in a methanol/water mixture effectively decreased particle aggregation, resulting in a reduction of particle size to as small as 6 nm.<sup>74</sup> This effect can be attributed to the electrostatic interactions between the protonated amine groups of L-lysine and the hydroxyl groups on the silica surface, which further delay the condensation process and enhance colloidal stability. The PEG-silane added to cover the silica surface was also found to attenuate the particle growth process by steric stabilization.<sup>74</sup> Co-surfactants have been additionally used as particle growth inhibitors for the same purpose.<sup>53</sup> Thus, adding the block copolymer Pluronic F127 ( $\text{EO}_{106}\text{-PO}_{70}\text{-EO}_{106}$ ) effectively stabilized the mesophase by quenching the condensation of silanol groups (Fig. 3).<sup>75</sup>

For instance, Kim *et al.* reported that the size of MCM-48-type particles, ranging from 70 to 500 nm, could be controlled by varying the amount of F127 used in the synthesis.<sup>76</sup> Similar results were achieved in the study of Bouchoucha *et al.*, in which the size of the MSNs was reduced from 300 to 90 nm by increasing the concentration of F127, ensuring high colloidal stability and minimal colloidal aggregation.<sup>73</sup>

Specifically in the context of oral drug delivery, Wang *et al.* investigated the effects of MSN size on mucus penetration and interaction with epithelial cells.<sup>77</sup> The authors prepared MSNs of different sizes (100 nm, 250 nm, and 480 nm) by adjusting the amount of F127 during synthesis. These particles were used as carriers for fenofibrate, a drug commonly prescribed to lower high cholesterol and triglyceride levels in the blood. Drug release profiles, along with transepithelial transport, degradation in gastric and intestinal fluids, and intestinal distribution of the formulated MSNs, were systematically studied and



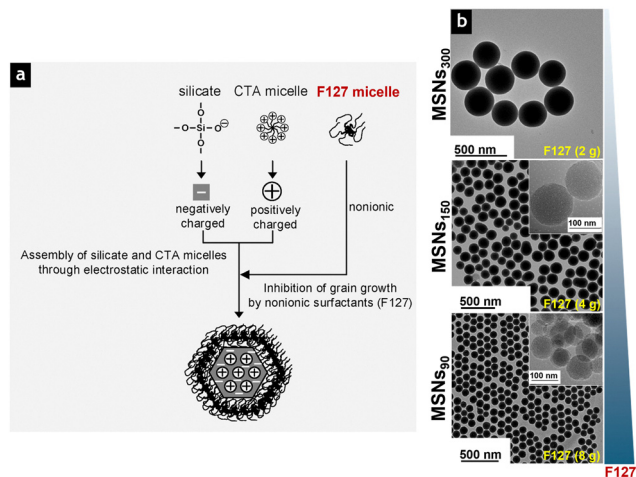


**Fig. 3** (a) Schematic representation of the inhibition of particle growth by adding Pluronic F127 as a co-surfactant in the synthesis of MSNs. Adapted with permission.<sup>75</sup> Copyright © 2006, American Chemical Society. (b) Transmission electron microscopy (TEM) images of MSNs synthesized by increasing the concentration of F127. Adapted with permission.<sup>73</sup> Copyright © 2016, American Chemical Society.

correlated with particle size. Among the tested materials, the medium-sized MSNs (250 nm) exhibited the best performance, with efficient cellular uptake and a low percentage of drug leakage in the intestinal tract. To further enhance particle stability under GI conditions and improve both mucus penetration and epithelial absorption, the MSN surface was modified with a bilayer consisting of polyethyleneimine (PEI)-coated carbon dots and PEG, which resulted in significantly improved oral bioavailability of fenofibrate.

## 2.2. Control of morphology

The morphology of MSNs is crucial to their performance, particularly in biological applications where shape-dependent interactions are complex and pivotal for ensuring particle bio-distribution, excretion, and relevant physiological responses.<sup>78,79</sup> While spherical MSNs have been extensively studied in recent years, significant advancements in controlling reaction conditions have unlocked the potential to obtain non-spherical rods, platelets, sheets, tubes, bundles, and cubes, which offer unique advantages for targeted applications (Fig. 4).<sup>52,80</sup>

The molar concentration of the base catalyst, surfactant, and TEOS influences the micelle assembly at the initial stage of the synthesis and affects the shape of the materials.<sup>52,85</sup> Therefore, Cai *et al.* diversified the morphology of MSNs by tuning the concentration of TEOS, base catalyst (NaOH or NH<sub>4</sub>OH), and CTAB, obtaining spherical, rod-shaped, and micrometer-sized oblate silica.<sup>86</sup> Several morphologies, such as spheres, shell-like, oval (or oblong), peanut-like, hollow, and complex yolk-shell structures, have also been obtained by adjusting the amount of dodecanol in combination with CTAB, used as a soft template mixture, under precise control of the temperature.<sup>87</sup>

Furthermore, organosilanes such as 3-aminopropyltrimethoxysilane (APTMS), allyltrimethoxysilane (ALTMS), and 3-isocyanatopropyltriethoxysilane (ICPTES) have been used in

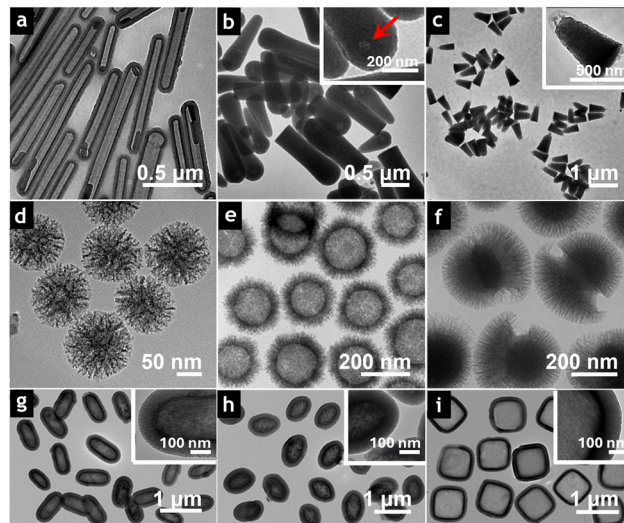


**Fig. 4** TEM images of silica particles exhibiting different morphologies: (a) tubular, (b) needle-shaped, and (c) bell-shaped, all obtained by varying the concentrations of ammonia, sodium citrate, polyvinylpyrrolidone, chloroauric acid, and/or NaCl during synthesis. Reprinted with permission.<sup>80</sup> Copyright © 2014, IOP Publishing Ltd. (d) DMSNs exhibiting central-radial pore structure. Reprinted with permission.<sup>81</sup> Copyright © 2013 American Chemical Society. (e) Hollow MSNs with spikes on the surface (silica nanopollens). Reprinted with permission.<sup>82</sup> Copyright © 2016 American Chemical Society. (f) Asymmetric head-tail DMSNs. The dendritic tail grows on spherical particles (head) using an oil/water emulsion system. The length and tail coverage on head particles are adjustable. Reprinted with permission.<sup>83</sup> Copyright © 2017 American Chemical Society. Nonspherical hollow MSNs with controlled morphologies: (g) capsules, (h) rice, and (i) cubes. The mesoporous structure grows by inheriting the original shape of the Fe<sub>2</sub>O<sub>3</sub> templates, which are subsequently removed to obtain hollow particles. Reprinted with permission.<sup>84</sup> © 2017 Wiley-VCH Verlag GmbH & Co. KGaA, Weinheim.

conjunction with silica precursors in co-condensation strategies to obtain spheres, rods, and hexagonal tubes.<sup>52</sup> This approach not only enabled the diversification of morphology but also facilitated silica functionalization. The change in the shape of MSNs was attributed to differential interactions between the alkoxy-silanes and the surfactant template.

Experimental conditions of sol-gel reactions can also be adjusted to finely tune the aspect ratio of the MSNs, which has driven the generation of rod-shaped particles.<sup>88</sup> Rod-shaped MSNs can be synthesized by increasing the amount of the base catalyst or by adding co-solvents such as heptane. Additionally, temperature variations have been found to produce elongated particles.<sup>89,90</sup> Rahmani *et al.* reported the generation of silica rods by adjusting the amount of ethanol used as a co-solvent in the sol-gel reaction, which facilitated control over the particle shape and mesoporous structure.<sup>91</sup> In an alternative procedure, Huang *et al.* described the synthesis of MSNs with diverse aspect ratios by condensing TEOS under low surfactant concentration.<sup>92</sup>

The aspect ratio of nanorods can be adjusted to optimize particular biological processes. Therefore, longer rods have shown efficient cellular internalization, while shorter ones have improved particle biodistribution.<sup>93–95</sup> Rod-shaped MSNs have exhibited enhanced interactions with biological interfaces,



such as cell membranes or extracellular matrices, potentially increasing therapeutic efficacy or diagnostic sensitivity.<sup>88,96,97</sup> The synthesis of rod-like MSNs has attracted significant interest for oral drug delivery due to their enhanced ability to overcome physiological barriers in the gut. This includes permeation through the mucus layer, cellular uptake, and interactions with the intestinal epithelium, which are particularly important when targeting oral drug delivery.<sup>47,92,93,96</sup> For example, in a recent study, Schmid *et al.* synthesized rod-shaped MSNs and evaluated the role of surface functionalization on particle biodistribution following oral administration *in vivo*.<sup>28</sup> The authors demonstrated the possibility of modulating the accumulation and retention of MSNs in the GI tract of mice through surface functionalization with PEG or hyaluronic acid (HA), highlighting the importance of the elongated shape of the rod-like MSNs in enabling potential penetration through the mucosal mesh.

Furthermore, Liu *et al.* reported significant advantages of rod-like MSNs for oral drug delivery due to their enhanced permeation and retention effects in mucus, which resulted in improved oral absorption of fenofibrate.<sup>98</sup> The authors tuned the aspect ratio of the MSNs and correlated the release kinetics of fenofibrate particle interaction with mucus with the morphology of the particles. Nanorods not only improved the oral bioavailability of fenofibrate compared to spherical particles but also enabled delayed drug release in simulated physiological media. In an alternative study, Zheng *et al.*<sup>47</sup> synthesized silica particles with varying aspect ratios but identical surface chemistry to investigate the effect of MSN shape on oral delivery. The authors reported that nanorods exhibited higher cellular uptake compared to spherical MSNs, primarily *via* caveolae-mediated endocytosis. In contrast, the uptake of nanospheres was mainly driven by a clathrin-dependent pathway. These findings confirmed that MSN morphology influences

their interactions with intestinal cells. Furthermore, the use of nanorods as carriers for doxorubicin hydrochloride significantly increased the drug's apparent permeability coefficient and improved its oral bioavailability *in vivo*.

### 2.3. Biphasic stratification approach for the synthesis of dendritic and virus-like MSNs

The precise control of the pore size of MSNs is crucial for biomedical applications involving the encapsulation and release of biomacromolecules.<sup>66</sup> Conventional MSNs typically exhibit pores smaller than 4 nm, which limits their use in this field. In contrast, DMSNs feature a unique central radial pore structure, which has attracted significant interest due to their unconventional open pore architectures, larger pores reaching up to 13 nm, and narrow particle size distributions that can be easily tailored by modifying the reaction conditions.<sup>99,100</sup>

Although there are several strategies for the synthesis of DMSNs, such as the organosilane-assisted co-condensation,<sup>99,100</sup> the heterogeneous oil-water biphasic stratification, reported by Shen *et al.* in 2014, is one of the most commonly used methodologies.<sup>101</sup> In this approach, TEOS is dispersed in a hydrophobic organic solvent, such as cyclohexane, cyclohexane, 1-octadecene, decahydronaphthalene, or toluene. At the same time, the surfactant (*e.g.*, CTAC) and the catalyst (*e.g.*, TEA) are added to the water phase. Under these conditions, the authors have proposed the formation of multigenerational and dendrimer-like center-radial mesopores through nucleation and growth processes driven by the self-assembly of silicate oligomers at the interfacial emulsion (Fig. 5). The research reported by Ernawati *et al.* supported the hypothesis that such microemulsion, spontaneously formed at the interface of water and oil, plays the main role in controlling the formation of hierarchical pores.<sup>100,102</sup> Therefore, by changing the organic solvent, the pore size has been increased from 2.8 to 13 nm.<sup>101</sup>

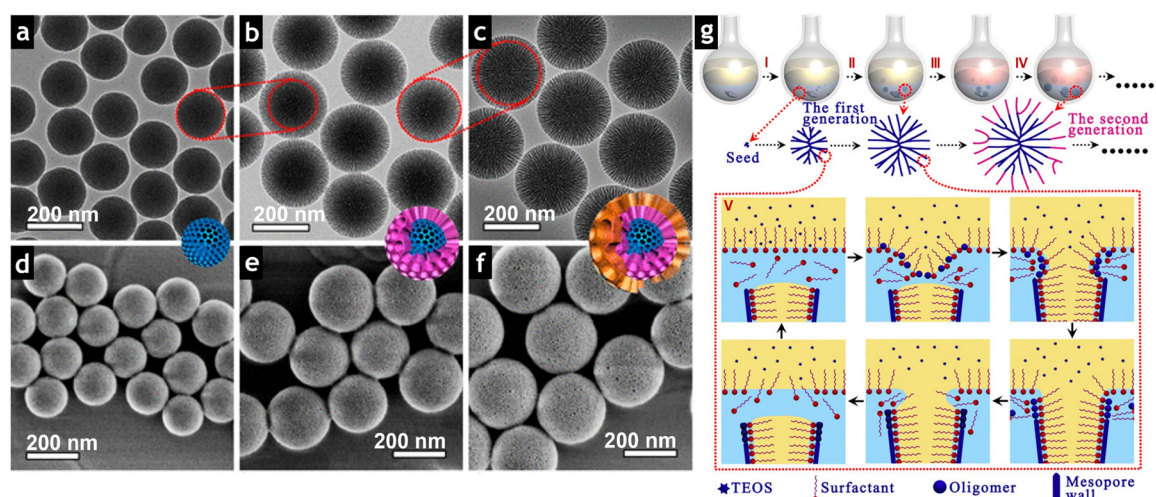


Fig. 5 TEM (a)–(c) and SEM (d)–(f) images of 3D-dendritic MSNs after the growth of one (a) and (d), two (b) and (e), and three particle generations (c) and (f) *via* the biphasic stratification approach. Scale bars stand for 200 nm. (g) Schematic representation of the formation of DMSNs and a hypothetical formation mechanism, including the nucleation of particles (I), the growth of the first DMSNs generation (II), the transformation of the upper oil phase (III), and the growth of the second DMSNs generation (IV). The mechanism of interfacial growth (V) shows the swelling of a single mesopore channel. Adapted with permission.<sup>101</sup> Copyright © 2014, American Chemical Society.



In the biphasic approach, surfactant concentration, stirring speed, temperature, and reaction time also influence the particle size and porosity of the DMSNs obtained.<sup>99</sup> Yu *et al.* reported the synthesis of dendritic particles by adding imidazolium ionic liquids (ILs) as co-surfactants and Pluronic F127 as a particle growth inhibitor.<sup>103</sup> The size of the DMSNs was precisely controlled within the 50–300 nm range by changing the alkyl chain length, IL concentration, and the amount of Pluronic F127.

The use of fluorocarbon anions as additives has also enabled a decrease in surface tension and interactions with cationic surfactants, resulting in finely tuned particle sizes (80–160 nm) and pore sizes (2–22 nm) by controlling the concentration of the additive.<sup>104,105</sup> In particular, the addition of sodium heptafluorobutyrate (FC4) to a typical biphasic system at room temperature favored the formation of large pores (>20 nm) and small-sized DMSNs (50 nm) compared to conventional synthesis at higher temperatures (*i.e.*, 80 °C).<sup>106</sup> The authors reported that increasing temperature induced particle growth (from 40 to 100 nm) with less influence on pore size expansion. Thus, a smaller ratio of FC4/CTAB was required to induce the growth of dendritic mesopores at room temperature.

The larger pore size of DMSNs compared to conventional MSNs has encouraged their application in the oral administration of peptide drugs and biologics.<sup>4,6,7</sup> For instance, Juère *et al.* adjusted the size and porosity of DMSNs by changing the organic co-solvent (*e.g.*, *n*-hexane, cyclohexane, or toluene) during the oil–water biphasic stratification reaction, aiming to optimize them for the oral delivery of insulin.<sup>14</sup> The use of DMSNs enabled the encapsulation of insulin within the silica mesopores with improved solubility and uptake by epithelial cells. Further combination of the insulin-loaded materials with succinylated  $\beta$ -lactoglobulin, a protein-based excipient, rendered pH-responsive tablets that prevented premature gastric release and controlled delivery in intestinal conditions.

DMSNs have also been explored as promising carrier candidates to overcome mucus clearance and epithelial barriers in the GI tract. In this context, Zhou *et al.* reported the use of PEGylated DMSNs to enhance mucus penetration and improve the permeation and intestinal absorption of andrographolide.<sup>107</sup> The authors synthesized the DMSNs using TEOS as the silica source, CTAB as the structure-directing agent, and sodium salicylate as the pore-expanding agent. The resulting DMSNs exhibited a spherical morphology (180–200 nm) with a well-defined central-radial dendritic structure and pore sizes of 24 nm, *i.e.*, large enough to encapsulate nanocrystal clusters of andrographolide. The hydrophilic nature of the functionalized DMSNs facilitated effective transepithelial transport and distribution within the intestinal tract. As a result, the oral bioavailability of andrographolide was significantly increased, while its anti-inflammatory activity was preserved, as demonstrated in both *in vitro* and *in vivo* studies.

Modifications of the heterogeneous oil–water biphasic stratification method have led to the synthesis of virus-like MSNs using CTAB in a cyclohexane/water biphasic system.<sup>99</sup> Wang *et al.* described the formation of these particles, characterized

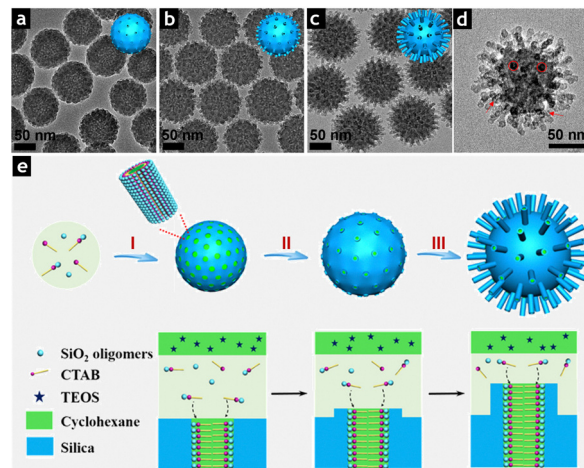


Fig. 6 TEM images of the MSNs obtained after (a) 24 h, (b) 26 h, and (c) 48 h reaction times in a biphasic system (cyclohexane/water) using a low CTAB concentration. (d) TEM image of a virus-like MSN; the red arrows and circles indicate the open tubular structures and their corresponding top views, respectively. (e) Schematic representation of the synthesis of virus-like MSNs and their suggested formation mechanism, including the formation and growth of spherical particles (I), the formation of the nucleation sites on the surface of the MSNs and the necks of the mesopore channels (II), and the orientated growth of the silica nanotubes (III). Adapted with permission.<sup>108</sup> Copyright © 2017, American Chemical Society.

by a spiky tubular rough surface through a single-micelle epitaxial growth approach (Fig. 6a–d).<sup>108</sup>

The authors proposed the formation of the virus-like particles from the isotropic growth of spherical MSNs under an ultralow concentration of surfactant template, followed by the oriented growth of silica nanotubes within the mesoporous channels (Fig. 6e). The resulting virus-like particles exhibited enhanced colloidal stability and uniform particle size, with core diameters ranging from 60 to 160 nm and outer “spike shell” diameters from 6 to 10 nm. By increasing the reaction time and adjusting the CTAB concentration, the tubular length of the spikes could be extended from 6 to 70 nm.<sup>99</sup>

Virus-like MSNs are considered a promising platform for vaccine development and targeted therapy. The increased surface roughness, which mimics the morphology of viral cell membranes, has promoted unique internalization pathways, extended blood circulation times, and efficient penetration through the mucus layer and permeation across the intestinal epithelium.<sup>96,109,110</sup> Indeed, a recent study by Cao *et al.* reported enhanced insulin permeability both *in vitro* and *in vivo* when the peptide drug was orally delivered in combination with virus-like MSNs (60 nm).<sup>111</sup> This effect was attributed to the reorganization of the TJJs, driven by the increased surface roughness of the virus-like particles compared to spherical Stöber MSNs. These findings offer a promising strategy for developing non-toxic permeation enhancers to improve the oral delivery of macromolecules. Furthermore, Sang *et al.*<sup>112</sup> reported the synthesis of core-shell MSNs (80 nm), functionalized with L-alanine and featuring virus-like nanospikes to enable chiral recognition for biomimetic drug delivery. These nanoparticles were used to encapsulate



indomethacin within their nanopores, enhancing both the solubility and stability of the drug. The virus-mimicking nanospikes improved mucus penetration and significantly increased the oral absorption of indomethacin.

#### 2.4. MSNs functionalization: general principles and tailored modification of the mesostructure

The modification of the porous network of mesoporous silica with organic functions allows for precise control over the surface chemistry of these materials. By tuning the surface of MSNs, interactions with target species, supports, or biological systems can be optimized, thereby favoring processes such as adsorption, desorption, molecular or ionic transports, and chemical interactions that are essential in drug delivery applications.<sup>113–116</sup>

The optimization of functionalization strategies has enabled the incorporation of a wide range of organic molecules, exposing diverse functional groups such as amines, phosphonates, carboxyl, hydroxyl, and alkyl chains.<sup>117</sup> These can be covalently anchored to the silica surface through co-condensation during synthesis or post-synthesis grafting. In the co-condensation approach, organic moieties are introduced *in situ* during the condensation of TEOS and functional silanes, such as alkoxy-organosilanes and chloro-organosilanes, in the presence of a surfactant template.<sup>118,119</sup> This process comprises the formation of a non-hydrolyzable covalent Si–C bond between the organosilane and the siloxanes formed, followed by the hydrolysis of these species to generate the silica network. On the other hand, if chemical modification is required exclusively on the outer surface of the material, it is possible to perform post-synthetic grafting followed by the removal of the surfactant template. Alternatively, the material could be directly calcined after synthesis and subsequently functionalized.<sup>120,121</sup>

On the other hand, organic molecules can be non-covalently adsorbed (*i.e.*, physisorbed).<sup>119</sup> For example, Schmid *et al.* recently reported the sequential loading of calcitonin, a hydrophilic peptide drug, into MSNs, followed by PEGylation to extend blood circulation time and minimize premature drug release from the mesopores.<sup>122</sup> The polymer chains were physically adsorbed onto the silica surface, effectively shielding drug-loaded MSNs from protein corona formation. PEGylated particles maintained colloidal stability and biofunctionality in the presence of serum proteins over time scales fully compatible with intravenous administration. These findings highlight the potential of adsorptive PEGylation as a straightforward and reproducible approach for drug loading and MSNs functionalization, enabling the development of cost-effective drug delivery formulations.

The incorporation of PEG to the silica network has also been reported through various alternative methodologies.<sup>123</sup> Due to their hydrophilic nature, the polymeric chains of PEG promote hydrogen bonding between water and ether groups, thus enhancing the biocompatibility of the grafted materials.<sup>124</sup> PEG has been covalently attached to MSNs to increase stealth properties, which prolong blood circulation times. Several strategies

were described by von Baeckmann *et al.* for this purpose, involving the prior modification of silica with functional silanes that subsequently reacted with PEG.<sup>125</sup> The coupling methods significantly influenced the grafting efficiency and the resulting protein adsorption, highlighting the importance of selecting an appropriate linking chemistry when aiming for surface functionalization. For example, in a recent study,  $\alpha$ -methoxy- $\omega$ -NHS polyethylene glycol (5056 Da) was grafted to rod-like MSNs *via* covalent coupling with amino moieties previously tethered on the silica surface.<sup>28</sup> PEGylation was aimed at increasing the residence time of the rods in the GI tract, which is particularly beneficial for treating inflammatory bowel disease (IBD). Indeed, upon oral administration to colitis-induced mice, the PEGylated particles were shown to accumulate in the lower intestinal tract, exhibiting low systemic absorption and clearance rates compared to other functionalized rod-like MSN tested.

Other hydrophilic polymers such as poly(*N*-isopropylacrylamide) and PEI have been used for MSNs functionalization, enabling long-term stability in biological media and improved biocompatibility.<sup>124</sup> Furthermore, the surface charge of MSNs have been modified with molecules bearing positive (*e.g.*,  $-\text{NH}_3^+$ ,  $-\text{NH}(\text{CH}_3)_2^+$ ) and negative (*e.g.*,  $-\text{COO}^-$ ,  $-\text{SO}_3^-$ ,  $-\text{PO}_3^-$ ,  $-\text{PCH}_3\text{O}_3^-$ ) functions, which results in colloidal stabilization (Fig. 7).<sup>124,126,127</sup>

The fine control of the surface charge of the silica has been widely explored to tune the electrostatic interactions of the material with adsorbed compounds. For example, functionalization with phosphonated silanes, such as 3-(trihydroxysilyl)propyl methylphosphonate (THMP), has considerably increased the negative surface charge of the modified MSNs, providing enhanced colloidal stability and cellular uptake.<sup>73</sup> MSNs have been alternatively modified with methylsilanes such as methyltrichlorosilane, trimethoxymethylsilane, and hexamethyldisilazane (HMDS) to tune the surface polarity, thus increasing hydrophobicity and interaction with cell membranes.<sup>128–130</sup>

Smart-functionalization strategies have also been employed to introduce moieties that modulate the release of adsorbed molecules, creating gate-keeping effects. These functions prevent desorption under specific conditions, effectively sealing the pores of silica. Furthermore, the responsive formulations enable controlled cargo release in response to external stimuli, such as changes in pH, redox processes, or enzymatic cleavage, which are particularly relevant in oral drug delivery.<sup>16,115</sup> For example, Popat *et al.* designed a bacterial enzyme-responsive delivery system for treating IBD.<sup>131</sup> The prodrug sulfasalazine (SZ), widely used in patients with IBD, was covalently attached to MCM-48 MSNs (spherical particles of 200 nm). Through interaction with azo-reductase, the anchored SZ molecules were reduced to 5-aminosalicylic acid (5-ASA), enabling the exclusive delivery of 5-ASA in the colon. Other pH-responsive formulations have been prepared for colon cancer therapy through the tailored functionalization of MSNs, confirming the versatility of such carriers for local drug delivery.<sup>132,133</sup>

There is a wide range of silane coupling agents containing reactive functional groups, such as *N*-hydroxysuccinimide (NHS),



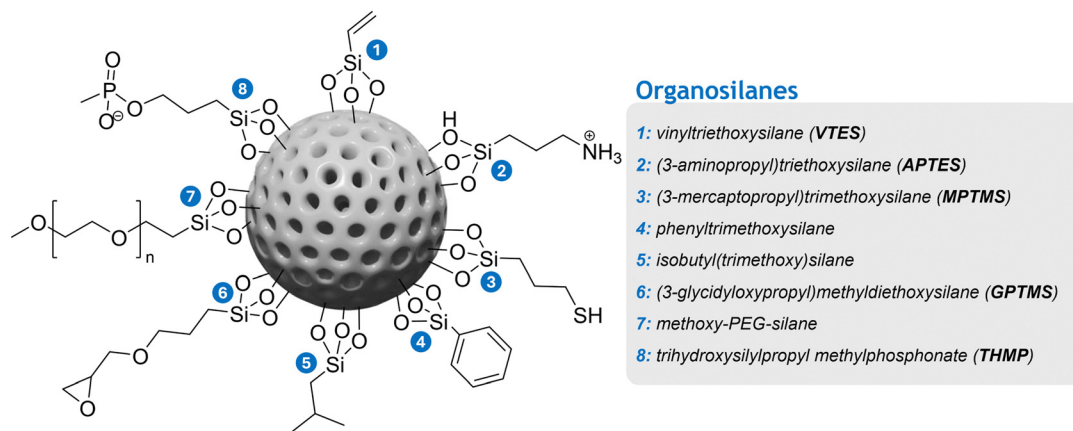


Fig. 7 Examples of organosilanes used for MSN functionalization.

isothiocyanates, epoxides, vinyl groups, and maleimides, which can be used to covalently link target compounds to MSNs. These coupling reactions can be conducted in water, organic solvents, or mixtures, offering great versatility for silica functionalization.<sup>16,115</sup> For example, 3-bromopropyltrichlorosilane has been grafted onto the surface of MSNs as a linker between silica and other organic molecules. The bromopropyl groups reacted then with sodium azide *via* nucleophilic substitution, a process formerly described as secondary grafting, resulting in azide-modified MSNs that were used for further functionalization through click reactions.<sup>134</sup> From this approach, Balamurugan *et al.* reported the subsequent conjugation of an alkyne-functionalized  $\alpha$ -helical polypeptide to the surface of the nanoparticles.<sup>135</sup> In a different strategy, Hohagen *et al.* reported linking chemistry strategies for functionalizing DMSNs with tannic acid, a water-soluble polyphenolic compound found in fruits, red wine, coffee, nuts, and beans.<sup>136</sup> Tannic acid-silane ligands were first obtained and inserted onto the particle surface using post-grafting procedures. The functionalization strategies included prior nucleophilic substitution reactions between tannic acid and the corresponding linker silanes, *e.g.*, (3-isopropyl)trimethoxysilane and (3-isocyanatopropyl)triethoxysilane. TANNylation enhanced the interactions of functionalized particles with intestinal cells, playing a crucial role in modulating biological responses, including endoplasmic reticulum signals that enable cell proliferation and resistance to metabolic stressors or sustained toxicity. These results greatly support the design and activity profiling of the TANNylated MSNs as nanocarriers for drug delivery applications.<sup>136</sup>

Beyond surface modifications for chemical diversification, the conjugation of biomolecules, such as proteins, polysaccharides, and lipids, to silica surfaces has been explored to improve biocompatibility, ensure targeted cellular uptake and drug delivery, enhance intestinal permeability, or protect oral formulations from harsh stomach conditions.<sup>30,137–140</sup> Although the covalent coupling of biomolecules to MSNs is not covered in this article, it is essential to note that they have ensured the retention of biological activity in the conjugated molecules,

which improves the stability and efficacy of the resulting bioconjugates.<sup>17</sup>

### 3. Connecting shape and surface chemistry with intestinal barrier function

Despite significant progress in designing silica nanocarriers to overcome GI barriers, the correlation between the properties of MSNs and their biological performance in the gut remains challenging, and many underlying mechanisms are still not fully understood. In this context, Iriarte-Mesa *et al.* conducted a systematic study to evaluate the influence of the morphology, size, and surface roughness of MSNs on their interactions with intestinal cells (Fig. 8a).<sup>96</sup> Leveraging the technological versatility of MSNs, the authors synthesized spherical (30, 90, and 130 nm), rod-shaped, and virus-like MSNs to evaluate their performance in a differentiated Caco-2/HT29-MTX-E12 cell co-culture model (Fig. 8b). This setup enabled the assessment of MSNs' penetration through the mucus layer and particle-cell interactions under conditions closely resembling key features of the intestinal compartment *in vivo*. These included the formation of villi-like structures, TJ expression, glucose transport, chloride regulation, and mucus secretion.<sup>141,142</sup> Such a study provides a comprehensive perspective on the topic, addressing aspects that have been extensively studied but lacked systematic and consensus-driven approaches.

Fluorescence live cell imaging was implemented to evaluate nanoparticle interactions with the intestinal cells and mucus. For the latter, a novel approach was introduced to assess the diffusion of MSNs through the complex mucin network, based on the analysis of the variations in the focal plane of fluorescent particles immediately after application to cells and after 6 h-treatment (Fig. 8c and d). This method provided a straightforward and reproducible alternative for the characterization of particle positioning in the cell monolayer, allowing for rapid and precise evaluation across multiple conditions. Moreover, confocal microscopy was used to assess particle-cell interactions,



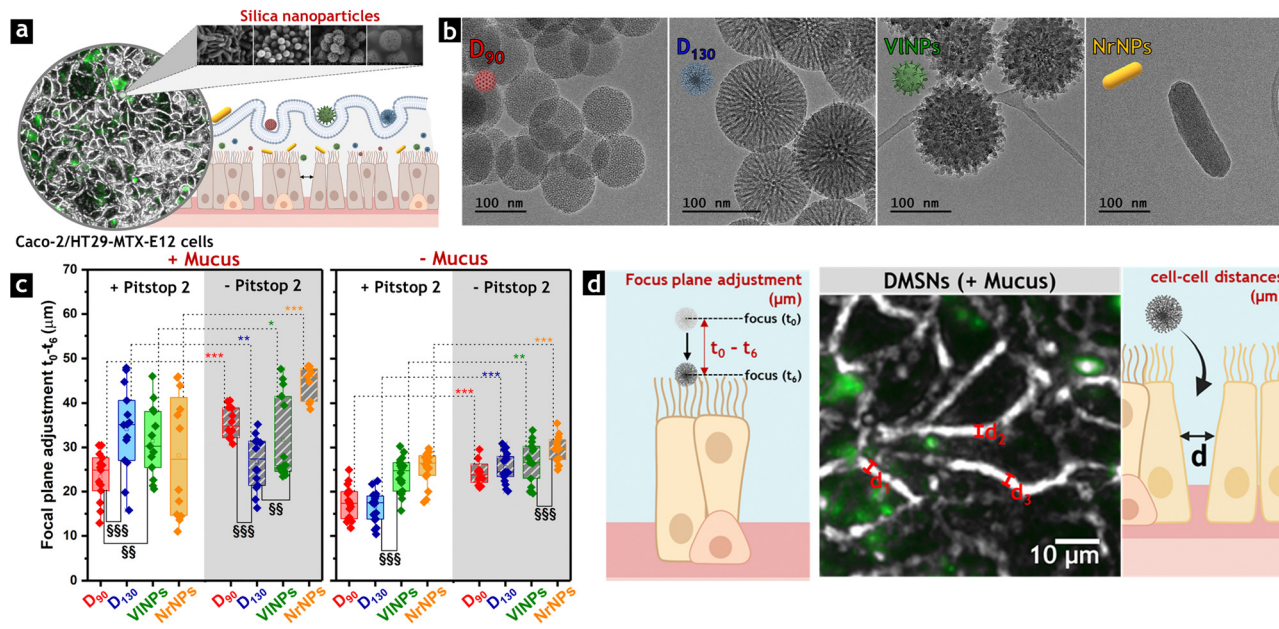


**Fig. 8** (a) Appearance of Caco-2/HT29-MTX-E12 cells used to evaluate morphology-dependent interactions of MSNs with intestinal cells. (b) Representative TEM images of the silica nanoparticles used in the study exhibiting spherical (D<sub>90</sub> and D<sub>130</sub>), virus-like (VINPs), and rod-shaped (NrNPs) morphologies. (c) Quantification of focal plane adjustment through fluorescence microscopy, based on the difference between optical parameters recorded immediately after treatment with FITC-labeled particles (t<sub>0</sub>) and after 6 h-incubation (t<sub>6</sub>) with or without the mucus layer (t<sub>0</sub> – t<sub>6</sub>). Reprinted under a CC-BY 4.0 license. Copyright © 2023 The Authors.<sup>96</sup> Published by American Chemical Society. (d) Graphical representations of the focal plane adjustment, correlated with particle penetration through the mucus layer, and the increased cell–cell distance triggered by particle treatments. Reprinted under a Creative Commons Attribution CC BY license. Copyright © 2024 The Author(s).<sup>143</sup> Small Science published by Wiley-VCH GmbH.

ensuring detailed biological characterization and validation of the quantification strategies implemented.

To investigate potential internalization pathways, the cells were pre-treated with Pitstop 2, a coated-pit inhibitor that blocks ligand access to the clathrin terminal domain and disrupts the nuclear pore complex (NPC) permeability barrier, a crucial step in endocytosis.<sup>40,144</sup> The significant decrease of particle–cell interactions in the presence of Pitstop 2 confirmed the crucial role of clathrin receptors in membrane adaptation to nanoparticulate materials, influencing membrane rigidity and biomechanical compliance upon exposure to MSNs. This observation was further supported by atomic force microscopy (AFM) analyses. Although MSNs were not internalized by intestinal cells, even in the absence of Pitstop 2, particle association with the outer cell membrane was observed, particularly depending on the morphology of the MSNs. Thus, among all tested materials, rod-shaped MSNs exhibited the strongest effects, increasing cell–cell distances without compromising monolayer integrity (Fig. 8d). Small particle size and surface roughness enabled similar MSNs diffusion through the mucus, albeit with limited association with the cell monolayer. In turn, the medium-sized spheres (130 nm) remained trapped in this layer due to a lack of colloidal stability, which reduced their contact with the intestinal cells.

To address the above limitations, the authors implemented diverse functionalization strategies in a follow-up study, tailoring the surface chemistry of this material (DMSNs, Fig. 9a),<sup>143</sup> that with 7.3 nm pores—significantly larger than those of other

produced MSNs (up to 2.8 nm)—was pointed out as a promising candidate for the encapsulation and subsequent delivery of peptide drugs and biologics. Thus, Iriarte-Mesa *et al.* applied post-grafting approaches to modify the DMSNs surface with PEG and phosphonate moieties (D-PEG and D-PO<sub>3</sub>, respectively), increasing particle hydrophilicity.<sup>143</sup> The latter modification further enhanced the negative surface charge of the DMSNs. In addition, the materials were functionalized with methyl and farnesol moieties, generating hydrophobic particles (D-CH<sub>3</sub> and D-Farn, respectively). As an alternative, phosphonate moieties were combined with methyl or farnesol groups, obtaining hybrid surface compositions (DPO<sub>3</sub>-CH<sub>3</sub> and DPO<sub>3</sub>-Farn). The same experimental setup was used to evaluate particle–cell interactions and diffusion through the mucus layer secreted by differentiated Caco-2/HT29-MTX-E12 cells, as observed *via* fluorescence microscopy.

The immunofluorescence staining of the TJs proteins ZO-1 and claudin-4 (CLND4) allowed for the evaluation of particle distribution on the cell monolayer and their effects on barrier integrity (Fig. 9b), correlating with the residual FITC fluorescence due to particle–cell interactions assed *via* live cell imaging (Fig. 9c), and further validating complementary quantification methodologies for the evaluation of the chemical surface–activity relationship.

The authors also performed immunostaining for the main mucin protein, MUC5AC, to enhance visualization of the particle distribution within the mucus layer and further confirmed their interaction with the cells in the absence of this barrier. This approach confirmed that hydrophilic particles with a



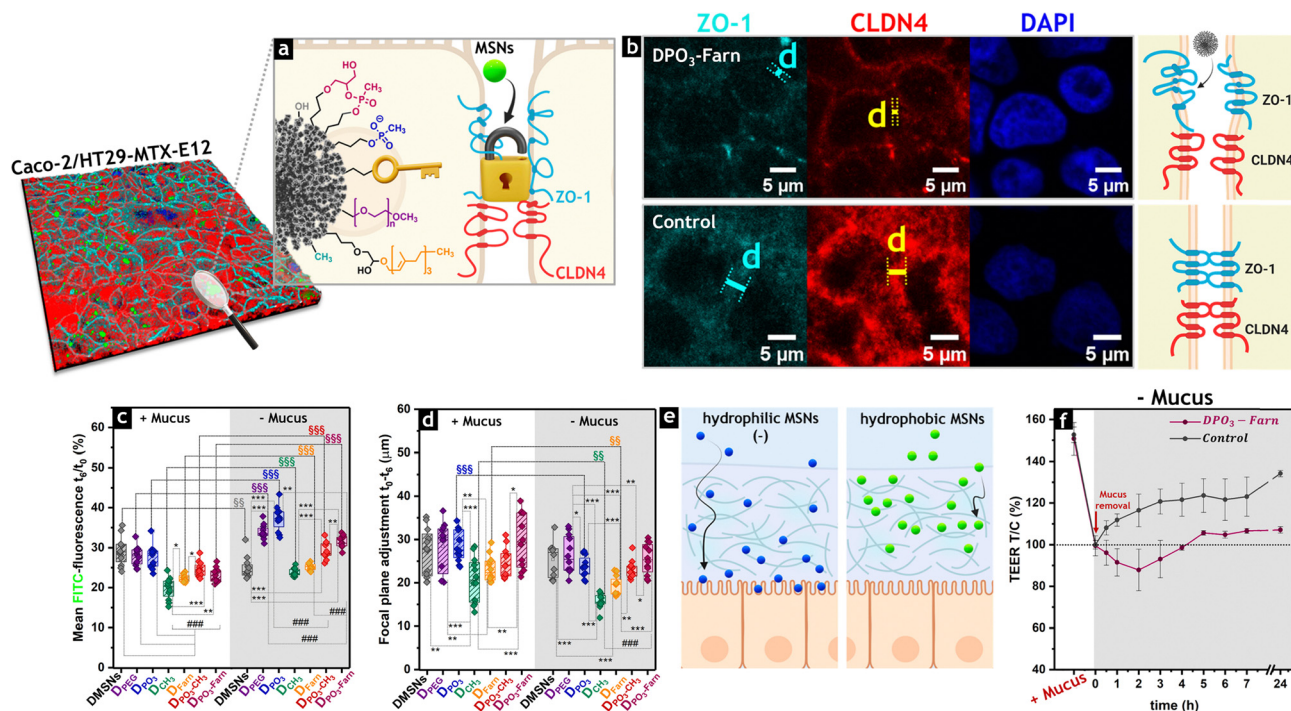


**Fig. 9** Diversification of surface chemistry of DMSNs for tailored interaction with intestinal cells (coculture cell model Caco-2/HT29-MTX-E12). Representative 3D reconstruction of the immunofluorescence staining of TJ proteins ZO-1 (cyan) and claudin-4 (CLDN4, red), showing the distribution of FITC-labelled MSNs throughout the cell monolayer. (b) Redistribution of ZO-1 (cyan) and CLDN4 (red) after 6 h-treatment with DPO<sub>3</sub>-Farn in the absence of mucus. Nuclei (stained with DAPI) are represented in blue. The control corresponds to non-treated cells. (c) Quantification of the residual FITC fluorescence resulting from particle–cell interactions, with and without the mucus layer, via live cell imaging. (d) Quantification of the focal plane adjustment obtained from the difference between the optical parameters set immediately after cell treatment with the FITC-labeled particles ( $t_0$ ) and after 6 h-incubation ( $t_6$ ) with and without the mucus layer ( $t_0 - t_6$ ). (e) Graphical representation of the particle diffusion through the mucus layer, depending on the surface chemistry. Created with <https://BioRender.com>. (f) Transepithelial electrical resistance (TEER) upon treatment with nonfluorescent DPO<sub>3</sub>-Farn in the absence of mucus, showing an increase in monolayer permeability in the presence of nanoparticles, followed by a gradual recovery after the first 2 h-incubation. Reprinted under a Creative Commons Attribution CC BY license. Copyright © 2024 The Author(s).<sup>143</sup> Small Science published by Wiley-VCH GmbH.

negative surface charge exhibited enhanced diffusion through the mucus. In contrast, hydrophobic MSNs strongly interact with mucins, becoming trapped and showing limited contact with the cell monolayer (Fig. 9d and e). No cytotoxic effects were observed across all tested conditions, both in the presence and absence of mucus, despite the transient barrier relapse detected upon treatment with hybrid DMSNs containing phosphonate and long carbon chain functions (DPO<sub>3</sub>-Farn). This response correlated with the reduction in transepithelial electrical resistance (Fig. 9f) and the reorganization of the TJ proteins ZO-1 and CLDN4 (Fig. 9b).

Interestingly, the diversification of the surface chemistry of DMSNs induced variations in the redistribution of TJs upon particle treatment. Thus, incubation with phosphonated particles increased cell–cell distances and reduced TJ expression (Fig. 9b). In contrast, DMSNs functionalized with methyl or farnesol groups induced lowered responses with negligible impact on intestinal permeability. These findings suggest that surface chemistry plays a key role in regulating particle–cell interactions, offering a potential strategy for modulating paracellular transport and expanding applications in both localized therapy in the gut and systemic drug delivery.

The increase in intestinal permeability upon treatment with phosphonated DMSNs further confirmed their potential for oral drug delivery via paracellular pathways. Furthermore, chemical modification of the cell membrane architecture, using the dietary lipid oleic acid (OA) and methyl- $\beta$ -cyclodextrin (m $\beta$ CD), provided deeper insights into particle–cell interactions, which were significantly influenced by the surface chemistry of the DMSNs. m $\beta$ CD facilitated cholesterol depletion, resulting in alterations in caveolae organization and membrane fluidity.<sup>145</sup> Meanwhile, OA rearranged the cytoskeleton of intestinal cells for the modulation of its structure and mechanotransduction.<sup>146</sup> These results confirmed both morphology- and chemistry-mediated responses and highlighted the complex relationship between MSN physicochemical properties and their biological performance in the gastrointestinal compartment. Both complementary studies provide a valuable overview of the tailored design of MSNs, offering useful tools for further mechanistic analyses.

### 3.1. Key considerations for the optimal design of MSNs for oral drug delivery

As reflected in the previous sections, recent advances in the design MSNs highlight the importance of fine-tuning their



physicochemical properties to overcome the complex biological barriers of the GI tract. Among the parameters evaluated in the studies reviewed in this perspective, morphology, surface roughness, particle size, and surface chemistry emerged as critical determinants of biological performance, specially to cross the mucosal barrier and interact with the tight intestinal epithelium (Fig. 10).

Rod-shaped and virus-like MSNs have exhibited improved penetration through the mucus layer (Fig. 10a) and more efficient contact with intestinal cells (Fig. 10b) compared to their spherical counterparts, which are more prone to mucus entrapment, particularly at larger sizes.<sup>96</sup> Increased surface roughness, as reported in virus-like MSNs, has promoted the reorganization of tight junction proteins, facilitating enhanced paracellular permeability.<sup>111</sup> Similar effects have been also observed for elongated nanorods with higher aspect ratios, which have significantly increased intestinal permeability and oral drug bioavailability.<sup>47,98</sup>

Surface chemistry has also proved to be a key factor in the rational design of mesoporous carriers for oral delivery.<sup>77,143</sup> Hydrophilic and negatively charged modifications have enhanced both mucus diffusion and epithelial contact (Fig. 10).<sup>30,107,143,147</sup> In contrast, non-polar hydrophobic coatings have led to strong interactions with mucins,<sup>49</sup> which hinder the efficient interaction with intestinal epithelium and cellular internalization consistently confirmed.<sup>148,149</sup> For this reason, the inclusion of amphiphilic moieties has been considered a promising alternative for effectively overcoming the mucosal barrier, transiently modulating epithelial barrier function.<sup>50,143,150</sup>

There are countless options for the synthesis and chemical modification of MSNs. The selection of the particle type and organic functional groups to be incorporated into the silica inorganic framework largely depends on the targeted application. Thus, while the local delivery approach focuses on promoting drug release within the intestinal lumen, systemic MSNs-based formulations would require efficient translocation of the carrier—either *via* transcellular or paracellular routes—to reach the blood

circulation, which might involve a different formulation design. Furthermore, during preparation of tailored mesoporous carriers additional aspects must be considered, including loading capacity, physicochemical stability of the confined cargoes, and drug-carrier interactions that modulate release kinetics, along with the potential inclusion of excipients (*e.g.*, binders, fillers, lubricants, and permeability enhancers) that contribute to overcome the harsh gastric environment, efflux transporters, metabolic enzymes in the intestinal wall, and microbiota, supporting optimal drug delivery.<sup>26,151</sup> Although MSNs porosity was not a primary focus of this perspective, it should also be carefully adjusted to ensure efficient drug encapsulation, which could have a critical role in drug solubility, stability and release.<sup>26,129,152,153</sup> Taken together, these aspects are essential to ensuring the success of MSN-based formulations for oral drug delivery.

## Conclusions

MSNs offer undeniable potential as carriers for peptide drugs and biologics. Their high drug-loading capacity, protective effects on encapsulated cargoes, and tunable physicochemical properties enable them to overcome gastrointestinal barriers, thereby expanding their applications in oral delivery. The studies reviewed here emphasize the critical influence of MSN morphology, size, and surface chemistry on their behavior in the intestinal compartment. While synthesis and functionalization strategies have significantly enhanced the performance of MSNs, challenges remain in achieving precise control over biocompatibility, stability, and drug release kinetics under physiological conditions. Future research should prioritize scalable and reproducible synthetic approaches, along with a deeper understanding of particle biodistribution, excretion pathways, and long-term toxicological effects. Addressing these aspects will boost the clinical translation of MSNs as drug nanocarriers, facilitating their integration into effective therapeutic solutions.

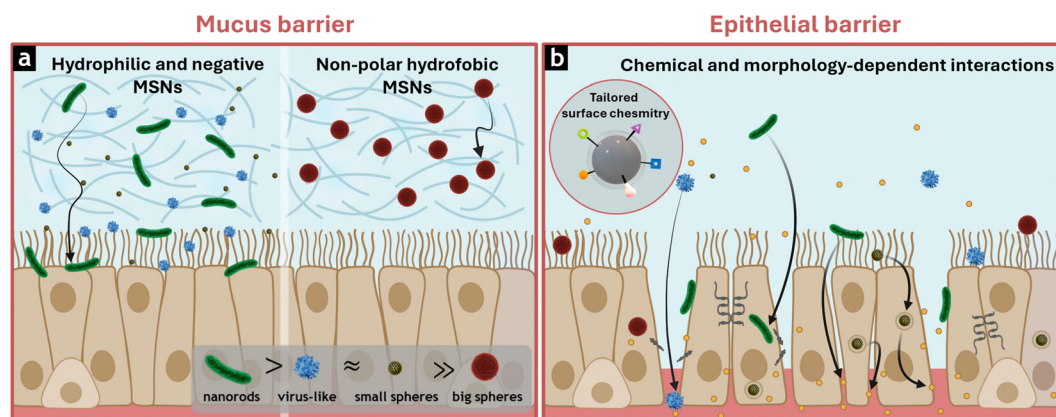


Fig. 10 Key features of tailored MSNs for overcoming the (a) mucus and (b) epithelial barriers through chemical- and morphology-dependent interactions with intestinal cells. These interactions facilitate oral drug delivery by enabling transient disruption of TJs, activation of transcellular transport pathways, and/or increased intercellular distances induced by mesoporous carriers. Created with <https://BioRender.com>.



## Author contributions

CIM conceptualized the perspective article and prepared the initial draft. FK contributed to the literature review, editing, and critical revisions. Both authors approved the final manuscript.

## Data availability

This perspective article does not involve the generation or analysis of new datasets. All data supporting the findings and discussions presented in this manuscript are derived from previously published studies, which are cited appropriately throughout the manuscript. For further details, please refer to the references cited.

## Conflicts of interest

There are no conflicts to declare.

## Acknowledgements

The authors would like to thank the University of Vienna (Austria) for the financial support. The authors would like to extend special thanks to Dr Giorgia Del Favero and Prof. Dr. Markus Muttenthaler (University of Vienna) for valuable discussions. Graphical elements included in the manuscript and table of contents were created with <https://BioRender.com>.

## References

- 1 K. Sharma, K. K. Sharma, A. Sharma and R. Jain, *Drug Discovery Today*, 2023, **28**, 103464.
- 2 R. Haider, *Asian J. Nat. Sci.*, 2023, **2**, 69–80.
- 3 L. Urquhart, *Nat. Rev. Drug Discovery*, 2019, **20**, 253.
- 4 T. D. Brown, K. A. Whitehead and S. Mitragotri, *Nat. Rev. Mater.*, 2020, **5**, 127–148.
- 5 P. Tyagi, S. Pechenov and J. Anand Subramony, *J. Controlled Release*, 2018, **287**, 167–176.
- 6 T. I. Janjua, Y. Cao, F. Kleitz, M. Linden, C. Yu and A. Popat, *Adv. Drug Delivery Rev.*, 2023, **203**, 115115.
- 7 M. M. Abeer, P. Rewatkar, Z. Qu, M. Talekar, F. Kleitz, R. Schmid, M. Lindén, T. Kumeria and A. Popat, *J. Controlled Release*, 2020, **326**, 544–555.
- 8 D. Wang, Q. Jiang, Z. Dong, T. Meng, F. Hu, J. Wang and H. Yuan, *Adv. Drug Delivery Rev.*, 2023, **203**, 115130.
- 9 A. Horowitz, S. D. Chanez-Paredes, X. Haest and J. R. Turner, *Nat. Rev. Gastroenterol. Hepatol.*, 2023, **20**, 417–432.
- 10 Y. Xiao, Z. Tang, J. Wang, C. Liu, N. Kong, O. C. Farokhzad and W. Tao, *Angew. Chem., Int. Ed.*, 2020, **59**, 19787–19795.
- 11 D. J. Drucker, *Nat. Rev. Drug Discovery*, 2020, **19**, 277–289.
- 12 Y. Cao, P. Rewatkar, R. Wang, S. Z. Hasnain, A. Popat and T. Kumeria, *Trends Pharmacol. Sci.*, 2021, **42**, 957–972.
- 13 A. Lérida-Viso, A. Estepa-Fernández, A. García-Fernández, V. Martí-Centelles and R. Martínez-Mañez, *Adv. Drug Delivery Rev.*, 2023, **201**, 115049.
- 14 E. Juère, R. Caillard, D. Marko, G. Del Favero and F. Kleitz, *Chem. – Eur. J.*, 2020, **26**, 5195–5199.
- 15 R. K. Kankala, Y. H. Han, J. Na, C. H. Lee, Z. Sun, S. B. Wang, T. Kimura, Y. S. Ok, Y. Yamauchi, A. Z. Chen and K. C. W. Wu, *Adv. Mater.*, 2020, **32**, 1907035.
- 16 A. Liberman, N. Mendez, W. C. Trogler and A. C. Kummel, *Surf. Sci. Rep.*, 2014, **69**, 132–158.
- 17 C. Iriarte-Mesa, M. Pretzler, C. von Baeckmann, H. Kählig, R. Krachler, A. Rompel and F. Kleitz, *J. Colloid Interface Sci.*, 2023, **646**, 413–425.
- 18 M. Lindén, *Enzymes*, 2018, **43**, 155–180.
- 19 C. Chelakkot, J. Ghim and S. H. Ryu, *Exp. Mol. Med.*, 2018, **50**, 1–9.
- 20 S. Liu, X. Wen, X. Zhang and S. Mao, *Expert Opin. Drug Delivery*, 2023, **20**, 1333–1347.
- 21 N. Sreeharsha, M. Philip, S. S. Krishna, V. Viswanad, R. K. Sahu, P. N. Shiroorkar, A. H. Aasif, S. Fattepur, S. M. B. Asdaq, A. B. Nair, M. Attimarad and K. N. Venugopala, *Coatings*, 2022, **12**, 358.
- 22 M. Vallet-Regí, F. Schüth, D. Lozano, M. Colilla and M. Manzano, *Chem. Soc. Rev.*, 2022, **51**, 5365–5451.
- 23 T. M. M. Ways, K. W. Ng, W. M. Lau and V. V. Khutoryanskiy, *Pharmaceutics*, 2020, **12**, 751.
- 24 A. K. Meka, A. Gopalakrishna, C. Iriarte-Mesa, P. Rewatkar, Z. Qu, X. Wu, Y. Cao, I. Prasad, T. I. Janjua, F. Kleitz, T. Kumeria and A. Popat, *Mol. Pharm.*, 2023, **20**, 2966–2977.
- 25 J. Leal, H. D. C. Smyth and D. Ghosh, *Int. J. Pharm.*, 2017, **532**, 555–572.
- 26 J. Florek, R. Caillard and F. Kleitz, *Nanoscale*, 2017, **9**, 15252–15277.
- 27 J. Lou, H. Duan, Q. Qin, Z. Teng, F. Gan, X. Zhou and X. Zhou, *Pharmaceutics*, 2023, **15**, 484.
- 28 R. Schmid, M. Volcic, S. Fischer, Z. Qu, H. Barth, A. Popat, F. Kirchhoff and M. Lindén, *Sci. Rep.*, 2023, **13**, 20175.
- 29 M. Yu, J. Wang, Y. Yang, C. Zhu, Q. Su, S. Guo, J. Sun, Y. Gan, X. Shi and H. Gao, *Nano Lett.*, 2016, **16**, 7176–7182.
- 30 Y. Zhang, M. Xiong, X. Ni, J. Wang, H. Rong, Y. Su, S. Yu, I. S. Mohammad, S. S. Y. Leung and H. Hu, *ACS Appl. Mater. Interfaces*, 2021, **13**, 18077–18088.
- 31 J. Wu, Z. Zhu, W. Liu, Y. Zhang, Y. Kang, J. Liu, C. Hu, R. Wang, M. Zhang, L. Chen and L. Shao, *ACS Nano*, 2022, **16**, 15627–15652.
- 32 B. Yameen, W. I. Choi, C. Vilos, A. Swami, J. Shi and O. C. Farokhzad, *J. Controlled Release*, 2014, **190**, 485–499.
- 33 A. Khalil, A. Barras, R. Boukherroub, C. L. Tseng, D. Devos, T. Burnouf, W. Neuhaus and S. Szunerits, *Nanoscale Horiz.*, 2024, **9**, 14–43.
- 34 J. Brunner, S. Ragupathy and G. Borchard, *Adv. Drug Delivery Rev.*, 2021, **171**, 266–288.
- 35 H. Gonschior, C. Schmied, R. E. Van der Veen, J. Eichhorst, N. Himmerkus, J. Piontek, D. Günzel, M. Bleich, M. Furuse, V. Haucke and M. Lehmann, *Nat. Commun.*, 2022, **13**, 4985.
- 36 I. Ramirez-Velez and B. Belardi, *Adv. Drug Delivery Rev.*, 2023, **199**, 114905.
- 37 Y. J. Hu, Y. D. Wang, F. Q. Tan and W. X. Yang, *Mol. Biol. Rep.*, 2013, **40**, 6123–6142.



- 38 N. G. Lamson, A. Berger, K. C. Fein and K. A. Whitehead, *Nat. Biomed. Eng.*, 2020, **4**, 84–96.
- 39 J. Nomme, A. Antanasijevic, M. Caffrey, C. M. Van Itallie, J. M. Anderson, A. S. Fanning and A. Lavie, *J. Biol. Chem.*, 2015, **290**, 16595–16606.
- 40 M. Sousa De Almeida, E. Susnik, B. Drasler, P. Taladriz-Blanco, A. Petri-Fink and B. Rothen-Rutishauser, *Chem. Soc. Rev.*, 2021, **50**, 5397–5434.
- 41 M. A. Deli, *Biochim. Biophys. Acta, Biomembr.*, 2009, **1788**, 892–910.
- 42 L. Delon, R. J. Gibson, C. A. Prestidge and B. Thierry, *J. Controlled Release*, 2022, **343**, 584–599.
- 43 W. H. Karasov, *J. Exp. Biol.*, 2017, **220**, 2495–2501.
- 44 V. Francia, C. Reker-Smit and A. Salvati, *Nano Lett.*, 2022, **22**, 3118–3124.
- 45 S. Moreno-Mendieta, D. Guillén, N. Vasquez-Martínez, R. Hernández-Pando, S. Sánchez and R. Rodríguez-Sanoja, *Pharm. Res.*, 2022, **39**, 1823–1849.
- 46 N. Means, C. K. Elechalawar, W. R. Chen, R. Bhattacharya and P. Mukherjee, *Mol. Aspects Med.*, 2022, **83**, 100993.
- 47 N. Zheng, J. Li, C. Xu, L. Xu, S. Li and L. Xu, *Artif. Cells, Nanomed., Biotechnol.*, 2018, **46**, 1132–1140.
- 48 X. Wang, Y. Qiu, M. Wang, C. Zhang, T. Zhang, H. Zhou, W. Zhao, W. Zhao, G. Xia and R. Shao, *Int. J. Nanomed.*, 2020, **15**, 9447–9467.
- 49 Y. Li, X. Chen and N. Gu, *J. Phys. Chem. B*, 2008, **112**, 16647–16653.
- 50 Y. Gao, Y. He, H. Zhang, Y. Zhang, T. Gao, J. H. Wang and S. Wang, *J. Colloid Interface Sci.*, 2021, **582**, 364–375.
- 51 Q. Huo, D. I. Margolese, U. Ciesla, P. Feng, T. E. Gier, P. Sieger, R. Leon, P. M. Petroff, F. Schüth and G. D. Stucky, *Nature*, 1994, **368**, 317–321.
- 52 R. Narayan, U. Y. Nayak, A. M. Raichur and S. Garg, *Pharmaceutics*, 2018, **10**, 118.
- 53 S.-H. Wu, C.-Y. Mou and H.-P. Lin, *Chem. Soc. Rev.*, 2013, **42**, 3862–3875.
- 54 B. G. Trewyn, I. I. Slowing, S. Giri, H. T. Chen and V. S.-Y. Lin, *Acc. Chem. Res.*, 2007, **40**, 846–853.
- 55 J. Patarin, B. Lebeau and R. Zana, *Curr. Opin. Colloid Interface Sci.*, 2002, **7**, 107–115.
- 56 F. Kleitz, W. Schmidt and F. Schüth, *Microporous Mesoporous Mater.*, 2001, **44–45**, 95–109.
- 57 C.-Y. Chen, H.-X. Li and M. E. Davis, *Microporous Mater.*, 1993, **2**, 17–26.
- 58 N. Lang and A. Tuel, *Chem. Mater.*, 2004, **16**, 1961–1966.
- 59 C. von Baeckmann, C. Eisen, H. Kählig, P. Guggenberger and F. Kleitz, *ChemCatChem*, 2021, **13**, 1140–1145.
- 60 M. Grün, I. Lauer and K. K. Unger, *Adv. Mater.*, 1997, **9**, 254–257.
- 61 W. Stöber, A. Fink and E. Bohn, *J. Colloid Interface Sci.*, 1968, **26**, 62–69.
- 62 P. P. Ghimire and M. Jaroniec, *J. Colloid Interface Sci.*, 2021, **584**, 838–865.
- 63 A. Saha, P. Mishra, G. Biswas and S. Bhakta, *RSC Adv.*, 2024, **14**, 11197–11216.
- 64 H. Li, X. Chen, D. Shen, F. Wu, R. Pleixats and J. Pan, *Nanoscale*, 2021, **13**, 15998–16016.
- 65 M. Manzano and M. Vallet-Regí, *Adv. Funct. Mater.*, 2020, **30**, 1902634.
- 66 V. Niculescu, *Front. Mater.*, 2020, **7**, 36.
- 67 F. Farjadian, A. Roointan, S. Mohammadi-Samani and M. Hosseini, *Chem. Eng. J.*, 2019, **359**, 684–705.
- 68 F. Rizzi, R. Castaldo, T. Latronico, P. Lasala, G. Gentile, M. Lavorgna, M. Striccoli, A. Agostiano, R. Comparelli, N. Depalo, M. L. Curri and E. Fanizza, *Molecules*, 2021, **26**, 4247.
- 69 N. A. Zainal, S. R. A. Shukor, H. A. A. Wabb and K. A. Razak, *Chem. Eng. Trans.*, 2013, **11**, 431–440.
- 70 Q. Chen, L. Han, C. Gao and S. Che, *Microporous Mesoporous Mater.*, 2010, **128**, 203–212.
- 71 A. H. Bari, R. B. Jundale and A. A. Kulkarni, *Chem. Eng. J.*, 2020, **398**, 125427.
- 72 K. Möller, J. Kobler and T. Bein, *Adv. Funct. Mater.*, 2007, **17**, 605–612.
- 73 M. Bouchoucha, M. F. Côté, R. C.-Gaudreault, M. A. Fortin and F. Kleitz, *Chem. Mater.*, 2016, **28**, 4243–4258.
- 74 K. Ma, U. Werner-Zwanziger, J. Zwanziger and U. Wiesner, *Chem. Mater.*, 2013, **25**, 677–691.
- 75 K. Ikari, K. Suzuki and H. Imai, *Langmuir*, 2006, **22**, 802–806.
- 76 T. Kim, P.-W. Chung and V. S.-Y. Lin, *Chem. Mater.*, 2010, **22**, 5093–5104.
- 77 Y. Wang, Y. Cui, Y. Zhao, Q. Zhao, B. He, Q. Zhang and S. Wang, *J. Colloid Interface Sci.*, 2018, **513**, 736–747.
- 78 N. Pal, J.-H. Lee and E.-B. Cho, *Nanomaterials*, 2020, **10**, 2122.
- 79 N. Hao, L. Li and F. Tang, *J. Biomed. Nanotechnol.*, 2014, **10**, 2508–2538.
- 80 A.-Q. Zhang, H.-J. Li, D.-J. Qian and M. Chen, *Nanotechnology*, 2014, **25**, 135608.
- 81 K. Zhang, L. L. Xu, J. G. Jiang, N. Calin, K. F. Lam, S. J. Zhang, H. H. Wu, G. D. Wu, B. Albela, L. Bonneviot and P. Wu, *J. Am. Chem. Soc.*, 2013, **135**, 2427–2430.
- 82 H. Song, Y. Ahmad Nor, M. Yu, Y. Yang, J. Zhang, H. Zhang, C. Xu, N. Mitter and C. Yu, *J. Am. Chem. Soc.*, 2016, **138**, 6455–6462.
- 83 P. L. Abbaraju, A. K. Meka, H. Song, Y. Yang, M. Jambhrunkar, J. Zhang, C. Xu, M. Yu and C. Yu, *J. Am. Chem. Soc.*, 2017, **139**, 6321–6328.
- 84 H. Geng, W. Chen, Z. P. Xu, G. Qian, J. An and H. Zhang, *Chem. – Eur. J.*, 2017, **23**, 10878–10885.
- 85 N. I. Vazquez, Z. Gonzalez, B. Ferrari and Y. Castro, *Bol. Soc. Esp. Ceram. Vidrio*, 2017, **56**(3), 139–145.
- 86 Q. Cai, Z. Luo, W. Pang, Y. Fan, X. Chen and F. Cui, *Chem. Mater.*, 2001, **13**, 258–263.
- 87 L. Han, Y. Zhou, T. He and G. Song, *J. Mater. Sci.*, 2013, **48**, 5718–5726.
- 88 S. Sargazi, U. Laraib, M. Barani, A. Rahdar, I. Fatima, M. Bilal, S. Pandey, R. K. Sharma and G. Z. Kyzas, *J. Mol. Struct.*, 2022, **1261**, 132922.
- 89 E. M. Björk, F. Söderlind and M. Odén, *Langmuir*, 2013, **29**, 13551–13561.
- 90 X. Pang, J. Gao and F. Tang, *J. Non-Cryst. Solids*, 2005, **351**, 1705–1709.



- 91 S. Rahmani, J. O. Durand, C. Charnay, L. Lichon, M. Férid, M. Garcia and M. Gary-Bobo, *Solid State Sci.*, 2017, **68**, 25–31.
- 92 X. Huang, X. Teng, D. Chen, F. Tang and J. He, *Biomaterials*, 2010, **31**, 438–448.
- 93 V. T. Cong, K. Gaus, R. D. Tilley and J. J. Gooding, *Expert Opin. Drug Delivery*, 2018, **15**, 881–892.
- 94 L. Li, T. Liu, C. Fu, L. Tan, X. Meng and H. Liu, *Nanomedicine*, 2015, **11**, 1915–1924.
- 95 X. Huang, L. Li, T. Liu, N. Hao, H. Liu, D. Chen and F. Tang, *ACS Nano*, 2011, **5**, 5390–5399.
- 96 C. Iriarte-Mesa, M. Jobst, J. Bergen, E. Kiss, R. Ryoo, J. C. Kim, F. Crudo, D. Marko, F. Kleitz and G. Del Favero, *Nano Lett.*, 2023, **23**, 7758–7766.
- 97 W. Borzęcka, P. M. R. Pereira, R. Fernandes, T. Trindade, T. Torres and J. P. C. Tomé, *J. Mater. Chem. B*, 2022, **10**, 3248–3259.
- 98 W. Liu, L. Zhang, Z. Dong, K. Liu, H. He, Y. Lu, W. Wu and J. Qi, *Nano Res.*, 2022, **15**, 9243–9252.
- 99 C. Xu, C. Lei, Y. Wang and C. Yu, *Angew. Chem.*, 2022, **61**, e202112752.
- 100 P. Hao, B. Peng, B. Q. Shan, T. Q. Yang and K. Zhang, *Nanoscale Adv.*, 2020, **2**, 1792–1810.
- 101 D. Shen, J. Yang, X. Li, L. Zhou, R. Zhang, W. Li, L. Chen, R. Wang, F. Zhang and D. Zhao, *Nano Lett.*, 2014, **14**, 923–932.
- 102 L. Ernawati, R. Balgis, T. Ogi and K. Okuyama, *Langmuir*, 2017, **33**, 783–790.
- 103 Y. Yu, J. Xing, J. Pang, S. Jiang, K. Lam, T. Yang, Q. Xue, K. Zhang and P. Wu, *ACS Appl. Mater. Interfaces*, 2014, **6**, 22655–22665.
- 104 Y. Wang, Y. A. Nor, H. Song, Y. Yang, C. Xu, M. Yu and C. Yu, *J. Mater. Chem. B*, 2016, **4**, 2646–2653.
- 105 M. Huang, L. Liu, S. Wang, H. Zhu, D. Wu, Z. Yu and S. Zhou, *Langmuir*, 2017, **33**, 519–526.
- 106 Y. Wang, H. Song, M. Yu, C. Xu, Y. Liu, J. Tang, Y. Yang and C. Yu, *J. Mater. Chem. B*, 2018, **6**, 4089–4095.
- 107 W. Zhou, B. Li, R. Min, Z. Zhang, G. Huang, Y. Chen, B. Shen, Q. Zheng and P. Yue, *Biomater. Sci.*, 2023, **11**, 1013–1030.
- 108 W. Wang, P. Wang, X. Tang, A. A. Elzatahry, S. Wang, D. Al-Dahyan, M. Zhao, C. Yao, C.-T. Hung, X. Zhu, T. Zhao, X. Li, F. Zhang and D. Zhao, *ACS Cent. Sci.*, 2017, **3**, 839–846.
- 109 Y. Feng, Y. Cao, Z. Qu, T. I. Janjua and A. Popat, *Pharmaceutics*, 2023, **15**, 2239.
- 110 S. M. Häffner, E. Parra-Ortiz, K. L. Browning, E. Jørgensen, M. W. A. Skoda, C. Montis, X. Li, D. Berti, D. Zhao and M. Malmsten, *ACS Nano*, 2021, **15**, 6787–6800.
- 111 Y. Cao, T. I. Janjua, Z. Qu, B. Draphoen, Y. Bai, M. Linden, M. Moniruzzaman, S. Z. Hasnain, T. Kumeria and A. Popat, *Biomater. Sci.*, 2023, **11**, 4508–4521.
- 112 Z. Sang, L. Xu, R. Ding, M. Wang, X. Yang, X. Li, B. Zhou, K. Gou, Y. Han, T. Liu, X. Chen, Y. Cheng, H. Yang and H. Li, *Nat. Commun.*, 2023, **14**, 7694.
- 113 M. Gisbert-Garzarán and M. Vallet-Regí, *Nanomaterials*, 2020, **10**, 916.
- 114 B. Singh, J. Na, M. Konarova, T. Wakihara, Y. Yamauchi, C. Salomon and M. B. Gawande, *Bull. Chem. Soc. Jpn.*, 2020, **93**, 1459–1496.
- 115 T. T. H. Thi, V. Du Cao, T. N. Q. Nguyen, D. T. Hoang, V. C. Ngo and D. H. Nguyen, *Mater. Sci. Eng., C*, 2019, **99**, 631–656.
- 116 B. Siddiqui, A. Rehman, I. Haq, A. A. Al-Dossary, A. Elaissari and N. Ahmed, *Int. J. Pharm.:X*, 2022, **4**, 100116.
- 117 R. P. Bagwe, L. R. Hilliard and W. Tan, *Langmuir*, 2006, **22**, 4357–4362.
- 118 J. A. S. Costa, R. A. De Jesus, D. O. Santos, J. B. Neris, R. T. Figueiredo and C. M. Paranhos, *J. Environ. Chem. Eng.*, 2021, **9**, 105259.
- 119 F. Hoffmann and M. Fröba, *Chem. Soc. Rev.*, 2011, **40**, 608–620.
- 120 C. Chircov, A. Spoială, C. Păun, L. Crăciun, D. Ficăi, A. Ficăi, E. Andronescu and S. C. Turculeț, *Molecules*, 2020, **25**, 3814.
- 121 D. Brühwiler, *Nanoscale*, 2010, **2**, 887–892.
- 122 R. Schmid, N. Neffgen and M. Lindén, *J. Colloid Interface Sci.*, 2023, **640**, 961–974.
- 123 J. S. Suk, Q. Xu, N. Kim, J. Hanes and L. M. Ensign, *Adv. Drug Delivery Rev.*, 2016, **99**, 28–51.
- 124 A. da Cruz Schneid, L. J. C. Albuquerque, G. B. Mondo, M. Ceolin, A. S. Picco and M. B. Cardoso, *J. Sol-Gel Sci. Technol.*, 2022, **102**, 41–62.
- 125 C. von Baeckmann, H. Kählig, M. Lindén and F. Kleitz, *J. Colloid Interface Sci.*, 2021, **589**, 453–461.
- 126 A. M. Putz, L. Almásy, A. Len and C. Ianăși, *Fullerenes, Nanotubes Carbon Nanostruct.*, 2019, **27**, 323–332.
- 127 V. Selvarajan, S. Obuobi and P. L. R. Ee, *Front. Chem.*, 2020, **8**, 602.
- 128 S. A. Kulkarni, S. B. Ogale and K. P. Vijayamohan, *J. Colloid Interface Sci.*, 2008, **318**, 372–379.
- 129 E. Juère, R. Caillard and F. Kleitz, *Microporous Mesoporous Mater.*, 2020, **306**, 110482.
- 130 E. Juère, G. Del Favero, F. Masse, D. Marko, A. Popat, J. Florek, R. Caillard and F. Kleitz, *Eur. J. Pharm. Biopharm.*, 2020, **151**, 171–180.
- 131 A. Popat, B. P. Ross, J. Liu, S. Jambhrunkar, F. Kleitz and S. Z. Qiao, *Angew. Chem., Int. Ed.*, 2012, **51**, 12486–12489.
- 132 Z. Qu, K. Y. Wong, M. Moniruzzaman, J. Begun, H. A. Santos, S. Z. Hasnain, T. Kumeria, M. A. McGuckin and A. Popat, *Adv. Ther.*, 2021, **4**, 2000165.
- 133 C. T. H. Nguyen, R. I. Webb, L. K. Lambert, E. Strounina, E. C. Lee, M.-O. Parat, M. A. McGuckin, A. Popat, P. J. Cabot and B. P. Ross, *ACS Appl. Mater. Interfaces*, 2017, **9**, 9470–9483.
- 134 R. Ranjan and W. J. Brittain, *Macromolecules*, 2007, **40**, 6217–6223.
- 135 S. S. Balamurugan, E. Soto-Cantu, R. Cueto and P. S. Russo, *Macromolecules*, 2010, **43**, 62–70.
- 136 M. Hohagen, P. Guggenberger, E. Kiss, H. Kählig, D. Marko, G. Del Favero and F. Kleitz, *J. Colloid Interface Sci.*, 2022, **623**, 962–973.
- 137 C. von Baeckmann, A. Riva, P. Guggenberger, H. Kählig, S. W. Han, D. Inan, G. Del Favero, D. Berry and F. Kleitz, *Adv. Mater. Interfaces*, 2022, **9**, 2102558.



- 138 R. Guillet-Nicolas, A. Papat, J. L. Bridot, G. Monteith, S. Z. Qiao and F. Kleitz, *Angew. Chem., Int. Ed.*, 2013, **52**, 2318–2322.
- 139 R. J. Mudakavi, A. M. Raichur and D. Chakravorty, *RSC Adv.*, 2014, **4**, 61160–61166.
- 140 L. Wang, W. Zhao and W. Tan, *Nano Res.*, 2008, **1**, 99–115.
- 141 P. Hoffmann, M. Burmester, M. Langeheine, R. Brehm, M. T. Empl, B. Seeger and G. Breves, *PLoS One*, 2021, **16**, 1–19.
- 142 O. Reale, A. Huguet and V. Fessard, *Chemosphere*, 2021, **273**, 128497.
- 143 C. Iriarte-Mesa, J. Bergen, K. Danielyan, F. Crudo, D. Marko, H. Kählig, G. Del Favero and F. Kleitz, *Small Sci.*, 2025, **5**, 2400112.
- 144 I. Liashkovich, D. Pasrednik, V. Prystopiuk, G. Rosso, H. Oberleithner and V. Shahin, *Sci. Rep.*, 2015, **5**, 9994.
- 145 G. Del Favero, F. Bialas, S. Grabher, A. Wittig, B. Bräuer, D. Gerthsen, C. Echalié, M. Kamalov, D. Marko and C. F. W. Becker, *Chem. Commun.*, 2019, **55**, 9649–9652.
- 146 J. Bergen, M. Karasova, A. Bileck, M. Pignitter, D. Marko, C. Gerner and G. Del Favero, *Arch. Toxicol.*, 2023, **97**, 1659–1675.
- 147 X. Tan, Y. Zhang, Q. Wang, T. Ren, J. Gou, W. Guo, T. Yin, H. He, Y. Zhang and X. Tang, *Biomater. Sci.*, 2019, **7**, 2934–2950.
- 148 P. Foroozandeh and A. A. Aziz, *Nanoscale Res. Lett.*, 2018, **13**, 339.
- 149 A. Kurtz-Chalot, J. P. Klein, J. Pourchez, D. Boudard, V. Bin, G. B. Alcantara, M. Martini, M. Cottier and V. Forest, *J. Nanopart. Res.*, 2014, **16**, 2738.
- 150 Y. Ma, Y. Guo, S. Liu, Y. Hu, C. Yang, G. Cheng, C. Xue, Y. Y. Zuo and B. Sun, *Nano Lett.*, 2023, **23**, 7552–7560.
- 151 S. Asad, A. C. Jacobsen and A. Teleki, *Curr. Opin. Chem. Eng.*, 2022, **38**, 100869.
- 152 R. Zhang, M. Hua, H. Liu and J. Li, *Mater. Sci. Eng., B*, 2021, **263**, 114835.
- 153 C. A. McCarthy, R. J. Ahern, R. Dontireddy, K. B. Ryan and A. M. Crean, *Expert Opin. Drug Delivery*, 2016, **13**, 93–108.

